TECHNIQUE FOCUS
Controlling Retention Time Drift in Industrial Settings

THEORY AND FUNDAMENTALS
Commercially Available Light Scattering Detectors for Size-Exclusion Chromatography

APPLICATIONS
Tools for Functional Assessment of Biotherapeutics

LC GC north america

solutions for separation scientists

Volume 39 Number 6 June 2021

www.chromatographyonline.com

LC
Loss of Efficiency from Extracolumn Dispersion in Tubing and Detectors

SAMPLES AND METHODS
BIOANALYSIS OF SMALL-MOLECULE DRUGS AND METABOLITES BY LC–MS

GC
How Water Affects Retention in PLOT GC Columns

Quantification of Adeno-Associated Virus Aggregation

The Field-Flow Fractionation Platform

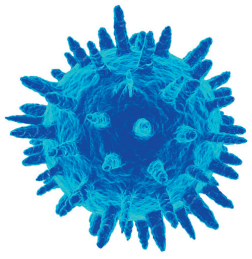

Adeno-associated viruses (AAVs) are increasingly used for gene therapy due to their versatility and safety. One of the biggest concerns for manufacturing a uniform AAV suspension is the presence of viral aggregates, which can create problems with transduction efficiency, biodistribution, and immunogenicity. These large AAV aggregates are challenging to separate and characterize by traditional column-based chromatography techniques such as size exclusion chromatography (SEC).

Asymmetrical Flow Field-Flow Fractionation with Multi Angle Light Scattering (AF4-MALS) can separate and size large AAV aggregates, and discern a difference in aggregate concentration due to the stressing protocol. Some or all of the large aggregates would be filtered out by SEC, resulting in incorrect determination of the aggregate content or the false conclusion that no aggregates are present.

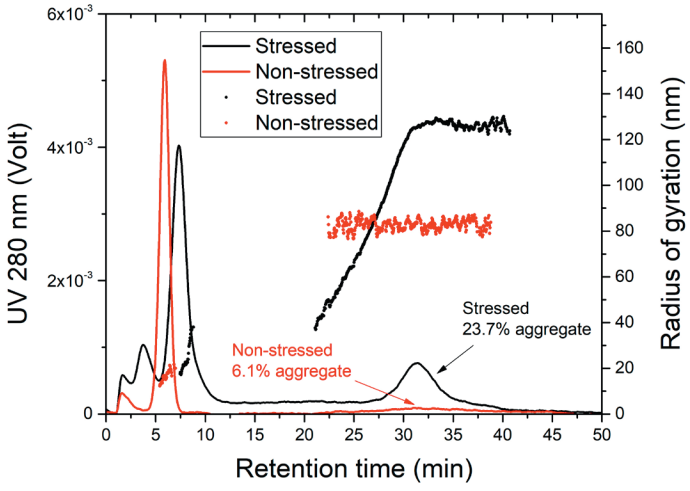

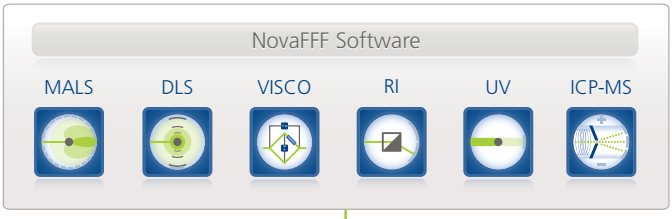

For more details visit www.postnova.com and search for 'virus'.

Contact us for more information: **www.postnova.com**

THEIRS is one-size-fits-all.
OURS has room to grow.

PEOPLE YOU CAN TRUST

Say goodbye to your comfort zone. **Learn more at ic.metrohmusa.com**

ION CHROMATOGRAPHY BY

Metrohm

LC GC north america

MANUSCRIPTS: For manuscript preparation guidelines, see chromatographyonline.com/lcgc-author-guidelines, or call The Editor, (732) 596-0276. *LCGC* welcomes unsolicited articles, manuscripts, photographs, illustrations, and other materials but cannot be held responsible for their safekeeping or return. Every precaution is taken to ensure accuracy, but *LCGC* cannot accept responsibility for the accuracy of information supplied herein or for any opinion expressed.

SUBSCRIPTIONS: For subscription and circulation information: *LCGC*, P.O. Box 457, Cranbury, NJ 08512-0457, or email mmhinfo@mmhgroup.com. Delivery of *LCGC* outside the United States is 14 days after printing. (*LCGC Europe* and *LCGC Asia Pacific* are available free of charge to users and specifiers of chromatographic equipment in Western Europe and Asia and Australia, respectively.)

CHANGE OF ADDRESS: Send change of address to *LCGC*, P.O. Box 457, Cranbury, NJ 08512-0457; alternately, send change via e-mail to mmhinfo@mmhgroup.com. Allow four to six weeks for change. PUBLICATIONS MAIL AGREEMENT No. 40612608. Return all undeliverable Canadian addresses to: IMEX Global Solutions, P.O. Box 25542, London, ON, N6C 6B2, CANADA. Canadian GST number: R-124213133RT001.

C.A.S.T. DATA AND LIST INFORMATION: Contact Melissa Stillwell, tel. (218) 740-6831, e-mail MStillwell@mmhgroup.com.
REPRINTS: Contact Michael J. Tessalone, e-mail: MTessalone@mjhlifesciences.com
INTERNATIONAL LICENSING: Contact Kim Scaffidi, e-mail: kscaffidi@mjhassoc.com

CUSTOMER INQUIRIES: Customer inquiries can be forwarded directly to MJH Life Sciences, Attn: Subscriptions, 2 Clarke Drive, Suite 100, Cranbury, NJ 08512; e-mail: mmhinfo@mmhgroup.com

Alliance for Audited Media

50% Recycled Paper 10-20% Post Consumer Waste

AN MJH life sciences™ BRAND

485F US Highway One South,
Suite 210
Iselin, NJ 08830
(732) 596-0276
Fax: (732) 647-1235

GAS TIGHT GC VALVES FROM THE COMPANY THAT INVENTED THEM

- For injection, stream selection and trapping
- Bores from 0.25mm (0.01") to 4mm (0.156")
- Zero dead volume fitting for 1/32", 1/16", 1/8" or 1/4" tubing
- Alloys and polymer composites to meet virtually any system requirement
- Manual, pneumatic or electric actuation

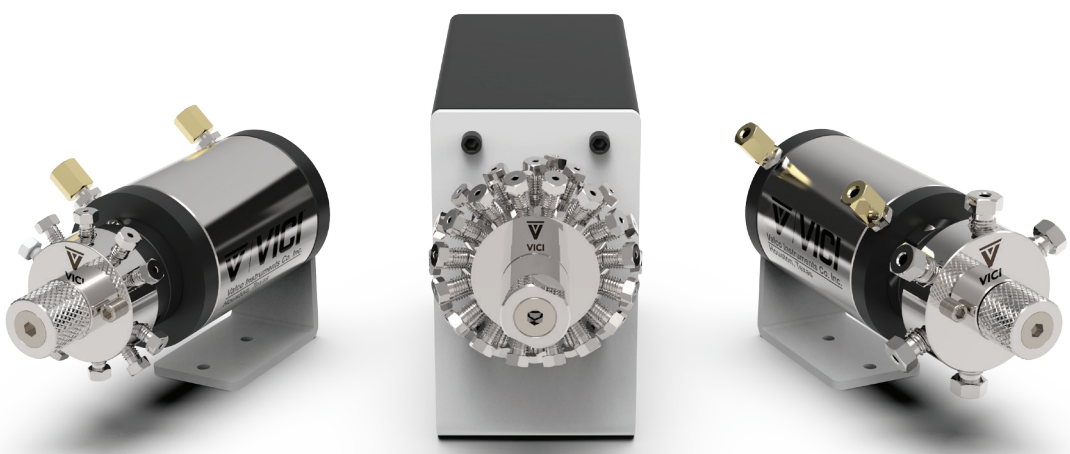

Scan the QR code to learn more about our GC valves

Learn More

VICI (800) 367-8424 sales_usa@vici.com

CONTENTS

LC GC north america

COLUMNS

PEER-REVIEWED ARTICLE

Cover Art: Image depicting analysis of drugs and their metabolites in blood and plasma

Cover image courtesy of stock.adobe.com/*Crystal light*

DEPARTMENTS

LCGC North America (ISSN 1527-5949 print) (ISSN 1939-1889 digital) is published monthly by MultiMedia Healthcare, LLC., 2 Clarke Drive, Suite 100, Cranbury, NJ 08512, and is distributed free of charge to users and specifiers of chromatographic equipment in the United States and Canada. LCGC is available on a paid subscription basis to nonqualified readers in the United States and its possessions at the rate of: 1 year (13 issues), $91.00; 2 years (26 issues), $163.00; in Canada and Mexico: 1 year (13 issues), $116.00; 2 years (26 issues), $182.00; in all other countries: 1 year (13 issues), $170.00; 2 years (26 issues), $304.00. Periodicals postage paid at Trenton, NJ 08650 and additional mailing offices. POSTMASTER: Please send address changes to LCGC, P.O. Box 457, Cranbury NJ 08512-0457. PUBLICATIONS MAIL AGREEMENT NO. 40612608, Return Undeliverable Canadian Addresses to: IMEX Global Solutions, P. O. Box 25542, London, ON N6C 6B2, CANADA Canadian GST number: R-124213133RT001. Printed in the USA.

Editorial Advisory Board

From the Chairman

Mike Hennessy, Sr.
Chairman & Founder, MJH Life Sciences

Many of our most popular articles in *LCGC* pertain to the pharmaceutical applications of chromatography. Accurate analytical methods are essential for ensuring the safety and efficacy of new therapeutics, and optimal approaches to analytical method development and use can reduce bottlenecks and thus help accelerate drug development. This issue features two such articles. Our "Perspectives in Modern HPLC" column introduces a series on the bioanalysis of small-molecule drugs and metabolites. This first installment of the series provides an overview, addressing the current trends in liquid chromatography and mass spectrometry techniques used in bioanalysis, including typical workflows, as well as key regulatory concerns that must be addressed. The "Focus on Biopharmaceutical Analysis" column addresses techniques for functional assessments of biologically derived therapeutics. Such assessments are particularly critical for biosimilars, where analytical testing must ensure functional comparability with the innovator product.

Other articles presented this month include the third part of the "LC Troubleshooting" column series on extra-column dispersion and its effect on performance within a liquid chromatography system. This installment continues the discussion of details of the contributions of specific system components, in this case focusing on dispersion that can occur in connecting tubing and detectors. The "Column Watch" column also provides troubleshooting help, in this case for gas chromatography. Guest authors Jaap de Zeeuw and Katarina Oden review of the effects of water on retention and selectivity in porous layer open tubular (PLOT) columns. This contribution concludes with some best practices that readers will find useful in preventing water from affecting their findings or to regenerate a column that has already been exposed to moisture.

Our peer-reviewed article continues Howard Barth's popular "Chromatography Fundamentals" series, with a summary of commercially available light scattering instrumentation with emphasis on new detector technology, to help readers understand the options. Given the complexity of data analysis involved in light-scattering detection, a glossary of principal symbols and a table of relevant relationships are also provided.

We hope you find the articles in this month's issue helpful in your work. Thanks for reading!

LC TROUBLESHOOTING

Where Has My Efficiency Gone? Impacts of Extracolumn Peak Broadening on Performance, Part III: Tubing and Detectors

Dispersion (broadening, or spreading) of analyte zones (peaks) outside of chromatography columns can seriously erode the resolution that good columns provide. In this installment, we focus on the contributions of dispersion in connecting tubing and detectors to the total level of extracolumn dispersion in a LC system.

Dwight R. Stoll and Ken Broeckhoven

In the installments of "LC Troubleshooting" from the last two months, we reviewed the basic concepts of extracolumn dispersion (ECD) (1), mentioned how the level of ECD associated with a particular instrument can impact the apparent quality of a separation (for example, as measured by resolution), and discussed dispersion associated with the injection step in some detail (2).

In this month's installment, we continue our discussion of details associated with the contributions of specific system components. Figure 1 illustrates the contributions of different system components to the total observed variance, starting with the injection step and ending with the detection step. In principle, the total observed peak variance is simply the sum of the variances contributed by each system component. This is only rigorously correct if the dispersion in each element of the system is independent of the others (3), but under most conditions, equation 1 is accurate enough to guide method development and system optimization (4). In this installment of "LC Troubleshooting," we continue by discussing dispersion in connecting tubing and detectors.

$$\sigma^2_{injection} = \sigma^2_{observed} + \sigma^2_{tubing,\ pre\text{-}col} + \sigma^2_{column} + \sigma^2_{tubing,\ post\text{-}col} + \sigma^2_{detection} \quad [1]$$

Dispersion in Connecting Tubing

It is a well known fact that increasing the length and inner diameter of connecting capillaries in a chromatographic instrument increases dispersion. This dispersion is the result of the parabolic flow profile that is established in an open capillary under laminar flow conditions. Under these conditions, the fluid in the center of the tube moves at twice the average velocity, whereas the fluid near the wall is stagnant (that is, stuck to the wall). Estimating the contribution of this dispersion that occurs in connecting capillaries to the total extracolumn band broadening in a liquid chromatography (LC) system is not straightforward. The two limiting conditions for which analytical solutions exist are as follows: 1) dispersion in a short, straight capillary at high-flow rates (with negligible radial equilibration between velocity streams); and 2) dispersion in very long capillaries at low-flow rates (that is, where full radial equilibration between velocity streams occurs by diffusion). In the first case, the dispersion contribution of the capillary is given by the Atwood-Golay equation below (5):

$$\sigma^2_{V,tub,AG} = \frac{\pi^2}{48} \cdot L^2_{tub}\, d^4_{tub} \quad [2]$$

where L_{tub} and d_{tub} are the length and diameter of the capillary, respectively. In the second case, the dispersion is given by the Taylor-Aris equation, where F is the flow rate through the capillary and D_m is diffusion coefficient of the analyte in the mobile phase (6).

$$\sigma^2_{V,tub,TA} = \frac{\pi}{384} \cdot \frac{F \cdot L_{tub} \cdot d^4_{tub}}{D_m} \quad [3]$$

Most conditions used for practical LC methods lie between the extreme conditions where equations 2 and 3 are valid, and thus require that we consider a partial radial equilibration of the analyte across the tubing diameter (that is, across different mobile phase velocity streams). For this purpose, we can use either a Giddings-style coupling of the previous expressions (equation 4) (7), or an exponential model based on numerical simulations (equation 5) (8):

$$\sigma^2_{v,tub} = \frac{\pi^2 \cdot L^2_{tub} \cdot d^4_{tub}}{48 + 384 \cdot \pi \cdot L_{tub} \cdot \frac{D_m}{F}} \quad [4]$$

$$\sigma^2_{V,tub} = \sigma^2_{V,tub,TA} \cdot \left[1 - \frac{1}{\alpha \cdot L_{tub}} \cdot (1 - e^{-\alpha \cdot L_{tub}})\right] \quad [5]$$

with α given by $\alpha = 15.04 \cdot \pi \cdot D_m / F$. In practice, however, equations 4 and 5 both seem to overestimate the degree of dispersion due to these capillaries in comparison to experimental observations, especially at high flow rates (7). One possible explanation for this observation comes from the fact that these equations are only valid for a straight tube, which is seldom used in real instruments where the capillaries are coiled and bent to fit in different instrument components, such as the injection valve, mobile phase pre-heaters, the column, and the detector inlet. As a result of this coiling, centripetal forces acting on the liquid cause secondary radial flow effects in the liquid. Beyond a critical flow rate, these radial flow effects are pronounced enough to enhance radial mixing and thus the equilibration of the analyte across the diameter of the tube. This in turn relaxes the axial dispersion that normally results from the parabolic flow profile. Nevertheless, equations 2–5 make it clear that using shorter and narrower capillaries reduces contribution of these tubes to the total extracolumn dispersion. This is especially true when using gradient elution, where the volumes of peaks exiting the column are typically much smaller than they are when using isocratic elution. Figure 2 shows that even for a relatively short (140 mm) piece of tubing between the column outlet and the detector inlet, the diameter of this tube can have a dramatic effect on peak width observed at the detector (3). When considering the use of narrow capillaries, however, one must be cautious about the pressure required to push the mobile phase through these tubes at the desired flow rate (ΔP_{tub}), because this increases along with the inverse fourth power of the column diameter as shown in equation 6 below (where η is the dynamic viscosity of the mobile phase).

$$\Delta P_{tub} = 128 \cdot \frac{\eta \cdot L_{tub} \cdot F}{\pi \cdot d_{tub}^4} \quad [6]$$

For example, changing from a commonly used 120 µm i.d. stainless steel capillary to a 75 µm i.d. capillary comes at the cost of a 6.5-fold higher pressure drop.

Dispersion in Detectors

Because of the widespread use of UV absorbance detectors in LC, most investigations into the contributions of detectors to extracolumn dispersion have been focused on UV detectors, although most fundamental aspects can also be applied to other types of detectors with flow-through detection cells. In a first, rough approximation, these flow cells behave as open-tubular flow paths that are either circular or rectangular in cross-section. As a result, the equations that govern dispersion in circular tubes can be used to estimate their contributions to extracolumn dispersion. However, the entire fluidic path in a detector mod-

Pharmaceutical Roots: The Origins of Opioids

Part 2 of the Pharmaceutical Roots content series from LGC Mikromol, investigates the natural origins of opioids, and offers a deeper dive into their uses, risks, and mechanisms of action.

Dulcie Phipps
Assistant Global Product Manager
LGC

Named after Morpheus, the Greek god of dreams, morphine is a type of opiate pain medication. It has played a vital role in the history of chemical neuroscience since its isolation in the 19th century. Morphine belongs to a class of chemical compounds called alkaloids, which are produced by many organisms. What makes morphine particularly interesting is that it is only produced in significant amounts by one plant—*Papaver somniferum,* or the Opium Poppy.

THE HISTORY OF OPIUM

The opium poppy is a member of *Papaveraceae*, a large family comprising over 700 species of flowering plants. The plants vary wildly from flower to flower, but all have in common the production of a milky substance designed to protect the plant from herbivores known as latex. The latex of *Papaveraceae* have a rich phytochemistry and, when dried, the milky-white latex produced by *P. somniferum* turns into a sticky, brown resin known as opium.

Opium can be smoked, eaten, or drunk, and evidence of humans using opium dates back over 5000 years. Despite this long history, it was not until the 16th century that opium was used medicinally in the Western world. Paracelsus, a Swiss-German alchemist, promoted the use of laudanum (from laudere, “to praise”), an extract of opium mixed with alcohol, for many ailments. Many variations of laudanum followed, and the concoctions were available without prescription until the early 20th century.

ISOLATION OF MORPHINE AND OTHER ALKALOIDS

In the early 1800s, the German pharmacist Friedrich Sertürner began experimenting with opium, succeeding in isolating morphine. Morphine accounts for around 10% of the total alkaloid content of opium and was the first alkaloid ever extracted from both opium and plants. Other alkaloids later isolated from opium include papaverine, noscapine, codeine and thebaine. Papaverine was discovered in 1848 by Georg Merck and is used to treat erectile dysfunction. Noscapine was first isolated in 1817 and sometimes used as a cough suppressant. Papaverine and noscapine have very different structures from morphine, codeine, and thebaine, and are neither psychoactive nor addictive.

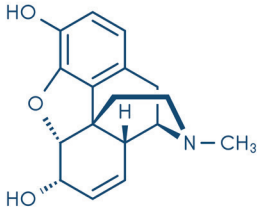

morphine

The French chemist Pierre Jean Robquet discovered codeine in 1832—he was also the isolator of noscapine. Codeine is less addictive and psychoactive than morphine or thebaine and is often used as a cough suppressant, or in conjunction with paracetamol as a painkiller. *P. orientalis* and *P. bracteatum* also produce thebaine, an important raw material for many opioids.

FROM OPIATES TO OPIOIDS

Opiates are the natural alkaloids obtained from the opium poppy. Unfortunately, many of these are highly addictive. Extensive research into semi-synthetic or synthetic opioids has been carried out, with hopes of finding a less addictive compound. As such, the opium family is a large one with semisynthetic opiate derivatives including oxycodone (from thebaine), hydrocodone (from codeine), and hydromorphone (from morphine) alongside opioid antagonists such as naloxone and naltrexone (both thebaine derivatives). There also exists a large number of synthetic opioids (almost 150) such as pethidine, fentanyl and methadone. Many of these compounds are less addictive but also less effective as analgesics, such as the cough suppressant pholcodine. Others, such as etorphine, are so potent they can be used to tranquilize elephants and walruses.

Perhaps the most infamous opioid is diacetylmorphine. In 1874, while on the hunt for a non-addictive morphine, English chemist Charles Wright boiled morphine and acetic anhydride, yielding diacetylmorphine. Wright carried out no further research on this compound and it was over 20 years later, in 1897, that German researcher Felix Hoffman re-discovered the acetylated substance. Bayer began marketing this new drug, calling it "Heroin" (based on the German "heroisch", meaning heroic), as a non-addictive morphine-alternative cough suppressant. Of course, it was soon realized that heroin was twice as potent as morphine with extremely high addiction rates, and its sale and production was banned.

LOOKING FORWARD

Although total synthesis of morphine has been realised, methods are not efficient enough to meet global demand. Opium poppies are still cultivated around the world, but there is ongoing research into new, potentially more efficient methods of obtaining opiates, by way of biosynthesis.

For over ten years, researchers in Montreal, Canada, have been attempting the genetic modification of yeast to synthesise bioactive molecules. By reconstructing plant pathways mediating synthesis of morphine precursor (S)-reticuline, they have been able to increase the amount of precursor produced and provide a platform for morphine synthesis. In other studies in Japan, researchers have manipulated strains of *Escherichia coli* to synthesise thebaine from increased production of (R)-reticuline. Although they have a long way to go, both groups have the aim of scaling the these platforms up to industrial level. Until then, we will have to rely on opium poppies.

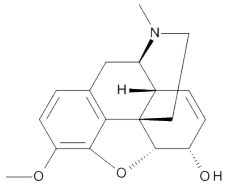

Codeine

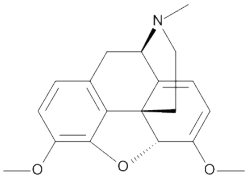

Thebine

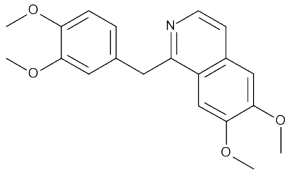

Papaverine

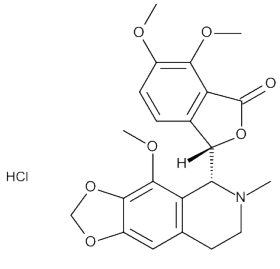

Noscapine

1. *Papaver orientalis* 2. *Paperver setigerum* 3. *Papaver somniferum* 4. *Papaver bracteum* 5. *Fumaria officinalis* 6. *Argemone mexicana*
Original artwork by Maddie Phipps.

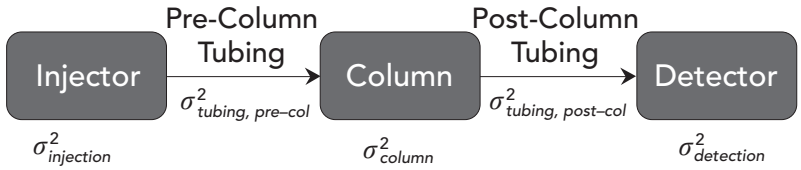

FIGURE 1: Illustration of the contributions of several LC system components to the total variance of peaks observed at the detector, $\sigma^2_{observed}$. We note that equation 1 is valid using either time- or volume-based variances.

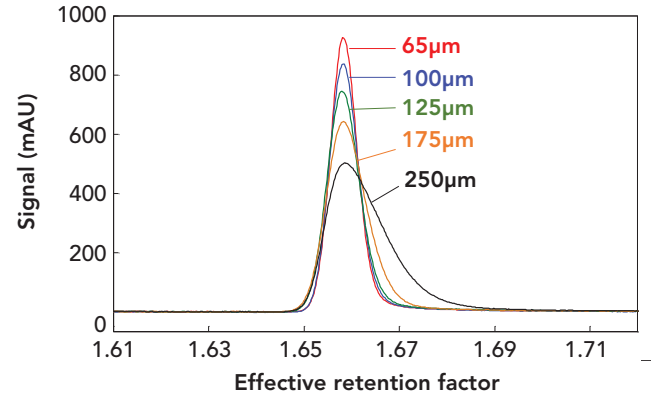

FIGURE 2: Example of the effect of post-column tubing diameter (L_{tub} = 140 mm in each case) on peak width and height in the case where gradient elution is used. The *x*-axis is effective retention factor ($[t_R\text{-}t_m]/t_m$). The column used was 50 mm x 2.1 mm i.d. (1.3 µm particles), the analyte was benzophenone, and the flow rate was 0.6 mL/min. Adapted from reference (4).

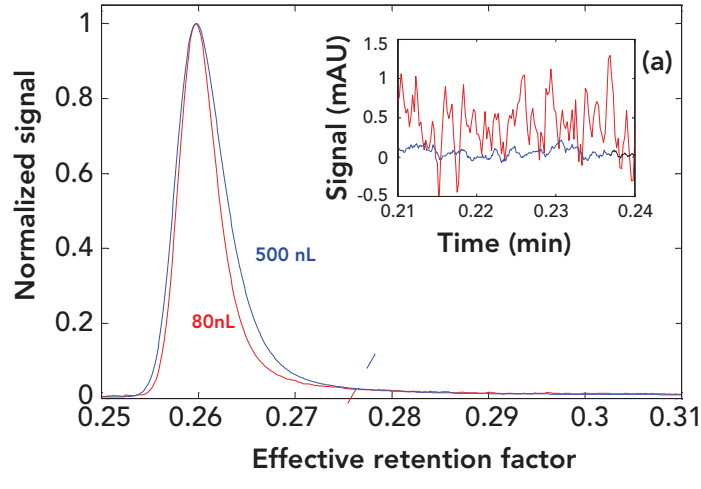

FIGURE 3: Comparison of peak width and baseline noise for UV flow cells with different volumes. (a) Inset shows the pre-peak region where the baseline noise is obviously much worse for the smaller flow cell. Note that the peak heights before normalization were about 360 and 560 mAU for the 80 and 500 nL flow cells, respectively. Adapted from reference (3).

ule is more than the detection cell itself, and often involves additional in- and outlet tubing, sharp turns, and changes in the cross-sectional area or shape of channels. Nevertheless, in the literature, the volumetric variance of dispersion attributed to the detector has often been related to the geometrical detection cell volume (V_{cell}) using an empirical relationship similar to that of the injection volume contribution (2).

$$\sigma^2_{V,detector} = \frac{V^2_{cell}}{\theta_{detector}} \quad [7]$$

The proportionality between cell volume and dispersion is not surprising because equations 2–5 show that a longer or broader flow path results in more dispersion. Thus, there is a tradeoff between dispersion and sensitivity during flow cell design because longer flow cells result in higher sensitivity (9), and broader cell design reduces signal noise. This is illustrated in Figure 3, which shows how narrower peaks are obtained using the flow cell with the smaller volume; however, this comes at the cost of reduced sensitivity (that is, lower peak height) and a much higher baseline noise level. Innovations in the fluidic and optical characteristics of these cells over the past decades have enabled improvements in sensitivity (higher) and noise (lower), while maintaining or decreasing flow cell volume.

Recent studies have shown that equation 7 provides poor estimates of the actual contributions of flow-through cells to the total extracolumn dispersion (10,11). As was discussed for the injection step (2), if a rectangular plug of analyte would move through the detector flow cell in a perfect plug flow without mixing, $\theta_{detector}$ would be 12. On the other hand, if the flow cell would behave as a "perfect mixer", $\theta_{detector}$ would be 1. However, if there are zones in the flow cell that are poorly swept because of flaws in the cell design, then values of $\theta_{detector}$ below 1 can be observed (10).

In addition, another consequence of the similarities between dispersion in a flow-through cell and dispersion in a capillary is that dispersion in the flow cell is expected to be flow rate dependent. Using a custom detector that allowed continuous variation of the cell pathlength, Dasgupta and others also showed that for short cell path lengths, the in- and outlet connections to the illuminated part of the flow cell make up the majority of the measured dispersion (10). To a first approximation, the dispersion at higher flow rates, typically above 0.5 mL/min, from modern low volume flow cells can be estimated using equation 7 with $\theta_{detector}$ = 0.5–0.8 (11). Given the fact that the dispersion of a flow cell is significantly affected by its internal design, some instrument vendors no longer report the geometrical cell volume, and instead report the expected contribution of the flow cell to peak widths (11).

In discussions on dispersion associated with detectors it is important to note that settings associated with the electronic components of the detector (for example, sampling frequency, and detector rise time or time constant) can also affect peak width and shape. Although strictly speaking these do not contribute to extracolumn dispersion in the same way as the other factors we have discussed (for example, detector cell volume), the effects of these settings can influence the observed peak variance and be confused with other contributions. Readers interested in learning more about this topic are referred to prior "LC Troubleshooting" articles (12), and some recent journal articles on the topic (13,14).

Finally, even though mass spectrometric (MS) detection is being used in more and more laboratories, there are far fewer studies of the contributions of MS detectors to extracolumn dispersion than there are for UV detectors (15,16). In the studies that have been done, however, it was found that when optimized MS settings are used, the ionization source and MS detector itself had little impact on observed peak widths. In fact, it was found that the tubing connecting the LC instrument to the mass spectrometer (MS) was the most critical contributor to the extracolumn dispersion for these hyphenated systems.

Summary

In this installment of "LC Troubleshooting," we have continued our discussion of details associated with the contributions of specific LC system components to extracolumn dispersion, this time focusing on connecting tubing and detectors. In the next installment in this series, we discuss how the impact of extracolumn dispersion can be different under isocratic and gradient elution conditions, and discuss the impact of post-column flow splitting on the total dispersion observed at the detector.

References

(1) D. Stoll and K. Broeckhoven, *LCGC N. Am.* **39**, 159–166, (2021).

(2) D. Stoll and K. Broeckhoven, *LCGC N. Am.* **39**, 208–213 (2021).

(3) G. Desmet and K. Broeckhoven, *Trends Anal. Chem.* **119**, 115619 (2019). https://doi.org/10.1016/j.trac.2019.115619

(4) K. Vanderlinden, K. Broeckhoven, Y. Vanderheyden, and G. Desmet, *J. Chromatogr. A* **1442**, 73–82 (2016). https://doi.org/10.1016/j.chroma.2016.03.016

(5) M.J.E. Golay and J.G. Atwood, *J. Chromatogr. A.* **186**, 353–370 (1979). https://doi.org/10.1016/S0021-9673(00)95261-0

(6) R. Aris, *Proc. R. Soc. Lond. A.* **235**, 67–77 (1956). https://doi.org/10.1098/rspa.1956.0065

(7) K.J. Fountain, U.D. Neue, E.S. Grumbach, and D.M. Diehl, *J. Chromatogr. A.* **1216**, 5979–5988 (2009). https://doi.org/10.1016/j.chroma.2009.06.044

(8) K. Broeckhoven and G. Desmet, *J. Chromatogr. A* **1216**, 1325–1337 (2009). https://doi.org/10.1016/j.chroma.2008.12.065

(9) M. Dong and J. Wysocki, *LCGC N. Am.* **37**, 750–759 (2019).

(10) P.K. Dasgupta, C.P. Shelor, A.F. Kadjo, and K.G. Kraiczek, *Anal. Chem.* **90**, 2063–2069 (2018). https://doi.org/10.1021/acs.analchem.7b04248

(11) K. Vanderlinden, G. Desmet, and K. Broeckhoven, *Chromatographia* **82**, 489–498 (2019). https://doi.org/10.1007/s10337-018-3622-1

(12) J.W. Dolan, *LCGC N. Am.* **14**, 378–380 (1996).

(13) M.F. Wahab, P.K. Dasgupta, A.F. Kadjo, and D.W. Armstrong, *Analytica Chimica Acta.* **907**, 31–44 (2016). https://doi.org/10.1016/j.aca.2015.11.043.

(14) A. Felinger, A. Kilár, and B. Boros, *Analytica Chimica Acta.* **854**, 178–182 (2015). https://doi.org/10.1016/j.aca.2014.11.014.

(15) D. Spaggiari, S. Fekete, P.J. Eugster, J.-L. Veuthey, L. Geiser, S. Rudaz, and D. Guillarme, *J. Chromatogr. A* **1310**, 45–55 (2013). https://doi.org/10.1016/j.chroma.2013.08.001.

(16) S. Buckenmaier, C.A. Miller, T. van de Goor, and M.M. Dittmann, *J. Chromatogr. A* **1377**, 64–74 (2015). https://doi.org/10.1016/j.chroma.2014.11.086.

ABOUT THE AUTHORS

Ken Broeckhoven received his PhD in 2010 from the Vrije Universiteit Brussel (VUB), in Brussels, Belgium. Following postdoctoral research at VUB and work as a visiting researcher in the separation processes laboratory at ETH Zurich, in Switzerland, he became a research professor at VUB in 2012. He was subsequently promoted to Assistant Professor and then to his current position as an Associate Professor in 2017.

ABOUT THE COLUMN EDITOR

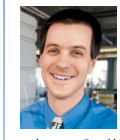

Dwight R. Stoll is the editor of "LC Troubleshooting." Stoll is a professor and the co-chair of chemistry at Gustavus Adolphus College in St. Peter, Minnesota. His primary research focus is on the development of 2D-LC for both targeted and untargeted analyses. He has authored or coauthored more than 75 peer-reviewed publications and four book chapters in separation science and more than 100 conference presentations. He is also a member of *LCGC*'s editorial advisory board. Direct correspondence to: LCGCedit@mmhgroup.com

COLUMN WATCH

Effects of Water on Adsorbents in Porous Layer Open Tubular (PLOT) Column Gas Chromatography (GC)

The best option for the gas chromatographic (GC) analysis of highly volatile analytes without cryogenic cooling is to use solid adsorbents. Open tubular GC columns with a deposited layer of solid adsorbent on the inside are known as *porous layer open tubular (PLOT)* columns. Adsorbents like molecular sieves, alumina, porous polymers, and even carbon materials are essential when analyzing light gases. Most gas samples contain water; although we are not interested in the amount of moisture that is present in the sample, water is injected onto the column unless a drying step of the sample is utilized. This article reviews the effects of water on retention and selectivity in gas–solid chromatography of various adsorbent PLOT columns.

Katarina Oden and Jaap de Zeeuw

Activated alumina has been studied as a chromatographic material for over 70 years. The high surface area of this porous material showed promise in separating C1–C5 hydrocarbons. Because of the extreme activity, tailing, and inconsistent responses of alumina, the material was at first considered almost unusable. In the mid-1950s, alumina oxides were deactivated with water vapor. This new approach drastically improved peak shape and provided consistent compound responses. However, water-deactivated alumina columns could be used only under isothermal conditions. The next significant improvement for porous alumina columns occurred in the 1970s when more stable deactivations with inorganic salts, such as potassium chloride (KCl), sodium sulfate (Na_2SO_4), and various proprietary salts, were implemented (1–3).

Even though the industry moved away from alumina-packed columns in favor of alumina-based porous layer open tubular (PLOT) columns, alumina columns remained a reliable choice for analyzing C1–C5 hydrocarbons. One thing has not changed since the 1950s—we still have problems with chromatography in the presence of moisture. To better understand the problematic effects of water on alumina columns, we studied the chromatographic behavior of C1–C5 hydrocarbons. Various selectivities of alumina deactivated PLOT columns were tested under the same isothermal chromatographic conditions. The analysis was performed again after injecting 0.1 µL of water onto the column, and the procedure was repeated five times.

Regardless of the column deactivation, the introduction of water onto the alumina PLOT column changes the retention time by accelerating the elution of the analytes. Water will act as a deactivating agent, meaning that the adsorption sites where water molecules are adsorbed will not be available for hydrocarbon retention. This process results in a decrease in retention time. Figures 1 and 2 show examples of the analysis of those two analytes, alumina MAPD (Figure 1) and alumina potassium chloride (Figure 2), as well as the analysis of the columns after exposing them to 0.5 µL of water in increments of 0.1 µL. Not only do we notice shifting retention times, but we also see changes in resolution, indicating that the polarity of the column has changed. Regardless of whether the column was deactivated with proprietary deactivation, MAPD, or potassium chloride, exposure to water decreases retention time and impacts the resolution of the compounds.

The introduction of any moisture to the column would further deactivate aluminum oxide, making the column less polar, which changes the column selectivity. The plotted deviation of retention indices of the analytes, which is based on the retention of adjacent *n*-hydrocarbons, confirms our observation. The analytes most affected by the moisture treatment over time are polar analytes—acetylene, propadiene, and methyl acetylene—that show more significant shifts in retention than the butanes and butenes (Figure 3). Similarly, the impact of moisture is more dramatic on a polar column, such as a sodium sulfate alumina column. Figure 4 illustrates changes in relative retention of acetylene on different types of deactivated alumina columns. The polarity of a sodium sulfate-deactivated alumina column declines considerably faster than a potassium chloride-deactivated alumina column. The potassium chloride-deactivated alumina has the lowest polarity, and it is the least sensitive to water.

Water will not damage the alumina column. The column can always be regenerated by conditioning it at the maximum temperature of the column.

Molecular Sieve 5A

Molecular sieves 5A (MSieve 5A) are zeolites, which are part of the family of aluminosilicate minerals. They are strong adsorbents with an unique, tunnel-like crystalline structure and a well-defined pore size. These strong adsorption properties make them ideal for analyzing permanent gases. The analytes separate on molecular sieves based on two mechanisms: First, how well the molecules fit into the material's pores, a separation based on the size of the molecules; and second, the physical interactions between the molecules and the MSieve 5A crystal, which is a separation that takes place based on the polarity. For example, nitrogen and oxygen are both small enough to fit in the pores of the 5A mineral, but oxygen, a smaller molecule than nitrogen, will navigate through the "tunnels" faster because it has less interactions with the pore surface and elutes from the column before nitrogen. In the case of carbon monoxide, dipole interactions play a more important role, and the MSieve 5A strongly retains these molecules. A bigger molecule, like sulfur hexafluoride (SF_6), will not be able to enter the pores of the zeolite. It will only be retained by the outside, free-accessible surface area. The same phenomena is observed with isoalkanes. Isobutane, for example, would be eluted around nitrogen at 40 °C, while *n*-butane (which can fit in the pores because of the linear structure), needs a very high temperature to be eluted (4,5).

Adsorption on molecular sieves is reversible, and the adsorption–desorption process is easily regulated with temperature. Molecular sieves are generally used as drying agents, and we know that we cannot analyze water using the MSieve 5A columns because of the high temperature required to desorb water from the molecular sieve pores. Our study on the effects of water on molecular sieves showed that the MSieve 5A has a relatively high tolerance to moisture in comparison to salt-deactivated alumina columns. A MSieve 5A PLOT column, with the dimensions of 30 m x 0.53 mm x 50 µm, was tested using a mixture of permanent gases at 40 °C. Afterward, water was injected onto the column at 100 °C isothermal. Column behavior was monitored by repeating the analysis of permanent gases at 40 °C. Figure 5 demonstrates a chromatogram of the initial analysis of permanent gases, black overlay, and blue overlay is a chromatogram after exposing the molecular sieves to water. The column had to be treated with 1 µL of water to see a notable shift in the retention time of the polar compound, which in this case is carbon monoxide.

Although 1 µL of water may seem like a small amount, the quantity is more signif-

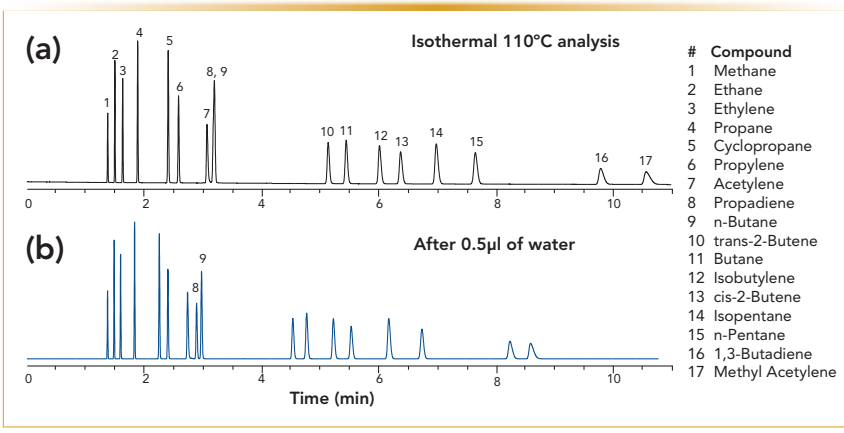

FIGURE 1: Comparison of the analysis of C1–C5 hydrocarbons on alumina MAPD deactivated column, 30 m x 0.32 mm x 5 µm, (a) chromatogram is the original analysis and (b) chromatogram after treating the column with 0.5 µL of water. Analysis conditions: carrier gas: helium at 5 mL/min, oven: 110 °C isothermal (*x*-axis is time in minutes, and *y*-axis is detector response).

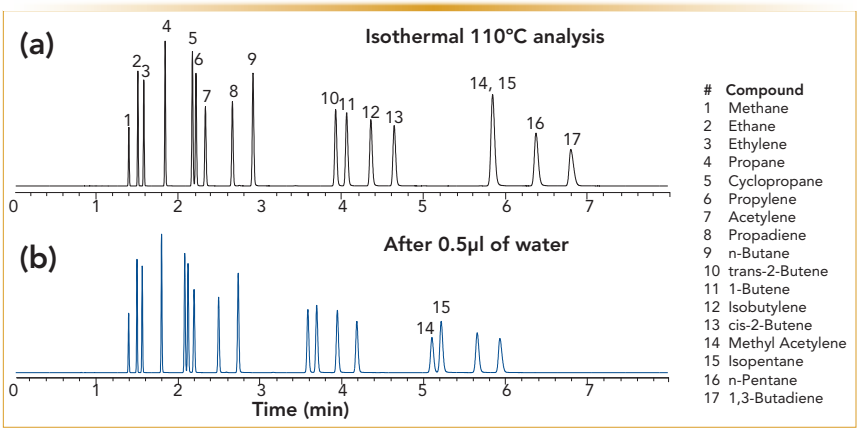

FIGURE 2: Comparison of analysis of C1–C5 hydrocarbons on a nonpolar alumina potassium chloride deactivated column, 30 m x 0.32 mm x 5 µm, (a) chromatogram is the original analysis and (b) chromatogram is after treating the column with 0.5 µL of water. Analysis conditions: carrier gas: helium at 5 mL/min, oven: 110 °C isothermal. (*x*-axis is time in minutes, and *y*-axis is the detector response).

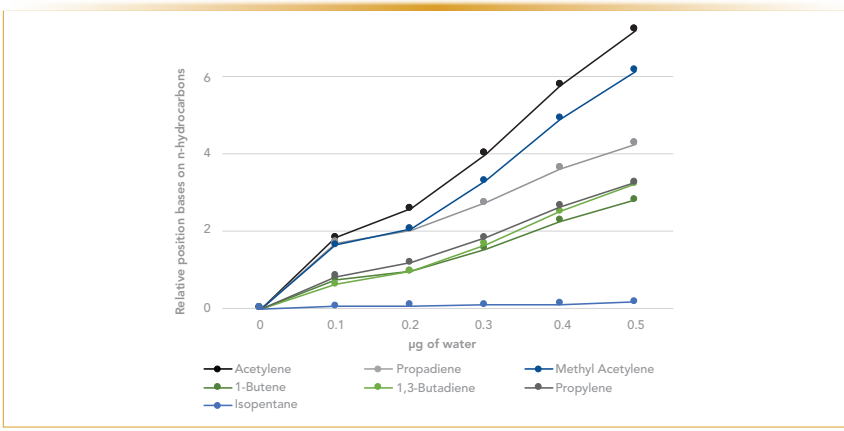

FIGURE 3: Relative behavior of analytes with the addition of water by monitoring deviation of retention indices of individual analyte on methyl acetylene and propadiene (MAPD) deactivated column.

icant when we look at it from a different angle. For example, if the gas sample has 50% relative humidity, with every 1 mL injection of gas, we are injecting ~0.01 µL of water onto the column. To see a slight shift of the carbon monoxide peak, we would need to make hundreds of injections.

Continued exposure of water to a MSieves 5A column will pack the adsorption sites with water. Figure 6 illustrates the changes in chromatography when the molecular sieves are treated with 50 µL of water at 100 °C. Retention times for all the analytes decrease, and some will be coeluted. When the peaks start to tail (Figure 6, blue overlay), that is an indicator that the column has reached its loading capacity partially because of the adsorbent sites being occupied with water.

The temperature necessary to desorb the water from the 5A molecular sieves is lower than the maximum temperature of the PLOT column. Therefore, water can be removed from the column. By conditioning the column at the maximum temperature of 300 °C, moisture is removed and initial performance is restored (Figure 7).

Porous Polymer PLOT Columns

Porous polymer PLOT columns are based on styrene-divinylbenzene (DVB-styrene) cross-linked polymers. They come in a range of polarities. For example, Q PLOT columns are made with 100% DVB-styrene polymers and are nonpolar. On the other hand, DVB-ethylene glycol-dimethyl acrylate PLOT columns, also referred to as *U PLOTs*, are highly polar (2,4).

Porous polymer PLOT columns are extremely versatile. They can separate a wide polarity range of molecules from gases to semi-volatiles. The main advantage of porous polymers is their hydrophobicity. Treating a column with large, continuous water injections does not have any effect on the adsorbent. Water elutes from the column very fast as a chromatographic peak and does

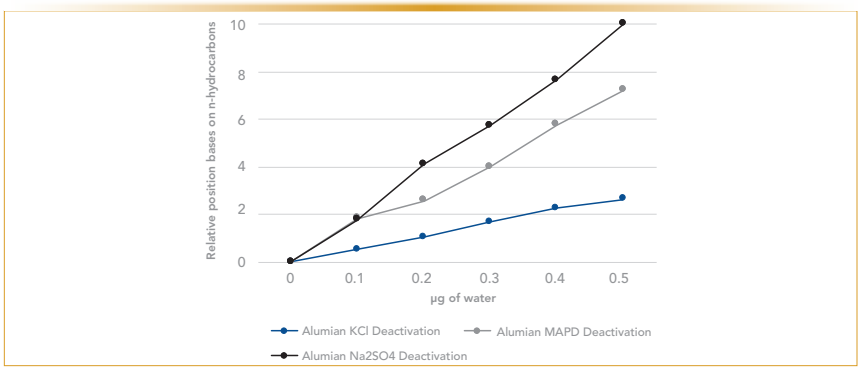

FIGURE 4: Behavior of acetylene. Comparison of changes of normalized retention after water treatment for all three deactivated columns. Water has the largest effect on a polar sodium sulfate deactivated column, followed by the methyl acetylene and propadiene (MAPD) deactivated column. The least affected is retention of acetylene on a potassium chloride deactivated column.

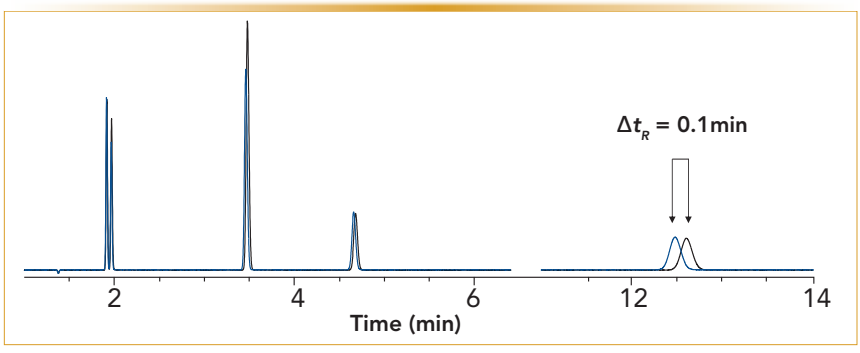

FIGURE 5: Chromatogram overlay of the analysis of permanent gases at 40 °C isothermal. The black overlay is the starting analysis, and the blue overlay is the analysis after exposing the MSieve 5A (30 m x 0.53 m x 50 µm) column to 1 µL of water. Peak identification is in order of elution: argon, oxygen, nitrogen, methane, and carbon monoxide. The retention time of carbon monoxide shifts after the column is treated with water. Analysis conditions are as follows: carrier gas, helium at 5 mL/min; and oven, 40 °C isothermal. (*x*-axis is the time in minutes, and *y*-axis is the detector response).

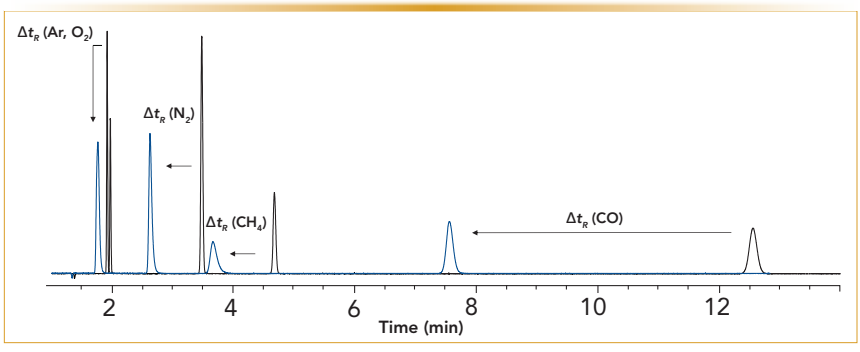

FIGURE 6: The overlay of the initial chromatogram of the analysis of permanent gases is in black, and the chromatogram after 50 µL of water was injected onto the column is in blue. Continued exposure of the MSieves 5A column to water will over time load the adsorption sites with water. Analysis conditions: carrier gas, helium at 5 mL/min; oven, 40 °C isothermal. (*x*-axis is the time in minutes, and *y*-axis is the detector response).

not change the selectivity of the column because of adsorption (Figure 8). This means there is no need to condition heat porous polymer columns to drive the water off, which reduces the downtime between injections.

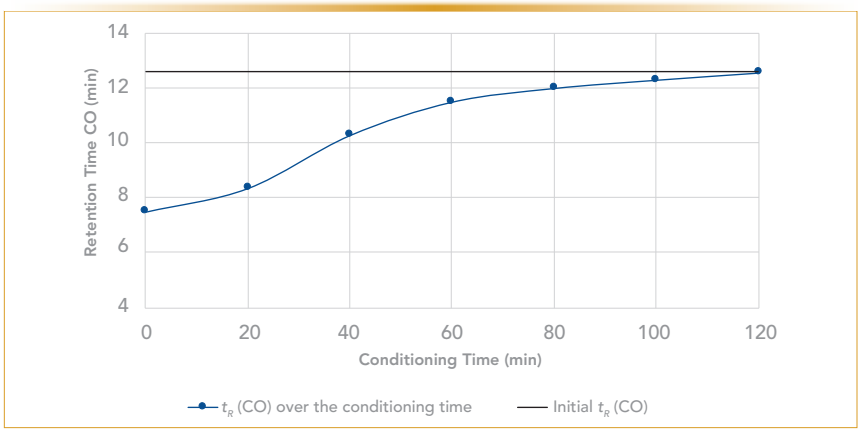

FIGURE 7: Graph of desorption process relative to the retention time (t_R) of the carbon monoxide (CO). The blue line is the original retention time, and the black line is the retention factor of CO over the conditioning time. Conditioning temperature is 300 °C.

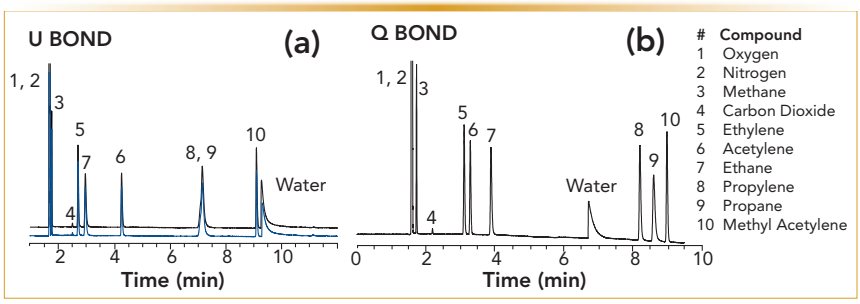

FIGURE 8: (a) U BOND: Overlay of analysis of permanent and hydrocarbon gases on a 30 m x 0.53 mm x 20 µm U BOND column before (black overlay) and after treating the column with 20 µL of water (blue overlay). Water elutes from the column as a chromatographic peak and does not change the column polarity. (b) Q BOND: Chromatogram of analysis of hydrocarbon gases with water using 30 m x 0.53 mm x 20 µm Q BOND. Depending on the polarity of the polymer water will be more or less adsorbed and elution time will change accordingly. Analysis conditions: Carrier gas, helium at 5mL/min; and oven, 40 °C (3 min) then 10 °C/min to 190 °C. (*x*-axis is the time in minutes, and *y*-axis is the detector response).

Conclusion and Final Tips

Although we deliberately exposed our columns to aliquots of water to illustrate the effect of water on adsorbent PLOT columns, systems with alumina and MSieves 5A PLOTs should be protected to keep water from causing slow but continuous deactivation and changes in column selectivity. To conclude this column, here are a few tips to keep in mind to prevent water from further affecting your chromatography or to regenerate your column if it has already been exposed to moisture:

1. If the moisture has already accumulated in the column, sodium sulfate-, potassium chloride-, or MAPD-deactivated alumina PLOT columns as well as MSieves 5A columns can be regenerated by conditioning the column at their maximum temperature.
2. Increasing the final temperature of the analysis to the maximum temperature of the column for 5–10 min will desorb the water during each analysis cycle.
3. However, it is always better to avoid water getting into the alumina column. By using a thick film, polar precolumn with a column-switching device, water and other impurities in the sample are backflushed and never enter the analytical column.
4. Gas samples can be dried using Nafion dryers, salt filters, cryogenic trapping, and preconcentrators. Water and other impurities in the sample are backflushed and never enter the column.

References

(1) L.R. Snyder and E.R. Fett, *J. Chromatog.*, **18**, 461–476 (1965).

(2) R.E. Majors and J. de Zeeuw, *LCGC N. Am.* **28**(10), 848–864 (2010).

(3) Z. Ji, R. Major, and E. Guthrie, *J. Chromatogr. A* **842**, 115 (1999).

(4) Colin Poole, *Gas Chromatography, 2nd Edition* (Wiley, New York, 2021).

(5) V.G. Berezkin and J. de Zeeuw, *Capillary gas adsorption chromatography (Chromatographic methods)* (Wiley, New York, 1996).

ABOUT THE CO-AUTHORS

Katarina Oden is an application chemist at Restek Corporation in Bellefonte, Pennsylvania.

Jaap de Zeeuw is the International Specialist Gas Chromatography at Restek Corporation in the Netherlands.

ABOUT THE AUTHOR

David S. Bell is a director of Research and Development at Restek. He also serves on the Editorial Advisory Board for LCGC and is the Editor for "Column Watch." Over the past 20 years, he has worked directly in the chromatography industry, focusing his efforts on the design, development, and application of chromatographic stationary phases to advance gas chromatography, liquid chromatography, and related hyphenated techniques. His main objectives have been to create and promote novel separation technologies and to conduct research on molecular interactions that contribute to retention and selectivity in an array of chromatographic processes. His research results have been presented in symposia worldwide, and have resulted in numerous peer-reviewed journal and trade magazine articles. Direct correspondence to: LCGCedit@mmhgroup.com

PERSPECTIVES IN MODERN HPLC

Bioanalysis of Small-Molecule Drugs and Metabolites in Physiological Samples by LC–MS, Part 1: An Overview

This article is the first of four on the bioanalysis of small-molecule drugs and metabolites by liquid chromatography–mass spectrometry (LC–MS). In this article, we provide an overview of the fundamentals, workflow, regulations, and modern trends on these quantitative assays.

Shashank Gorityala, David Roos, and Michael W. Dong

Bioanalysis is the term used to describe the quantitative assessment of drugs and their metabolites in biological fluids (such as blood, plasma, and urine) and tissue homogenates. Bioanalysis plays a pivotal role in the research, discovery, development, and commercialization of new drug therapeutics, and also offers many career opportunities for analytical chemists. Initially, bioanalysis was first used to detect illicit drugs in biological fluids to investigate overdosing in forensic cases. The field then grew from there with the development of pharmacokinetic science (1).

The four white papers for this planned series are:

- Part 1: An overview of the fundamentals and regulations.
- Part 2: Sample preparation for different sample types.
- Part 3: Method development–optimization and best practices.
- Part 4: Method validation for regulated bioanalysis.

Part 1 focuses on the bioanalysis of new chemical entities (NCE) in physiological fluids by liquid chromatography–mass spectrometry (LC–MS) in nonclinical and clinical samples. It strives to be a primer for the novice and a guide to the fundamentals of methodologies and regulations for the laboratory scientist. Bioanalysis of large-molecule biotherapeutics is not covered in this part. LC–MS applications and methodologies in biochemical research, drug metabolism, biomarker analysis, and clinical diagnostics are briefly mentioned.

Table I lists the common acronyms and brief definitions. Some terms are further described in the text or cited in references. For comprehensive explanations, the reader is referred to books and articles on drug development, pharmacology, pharmacokinetics (PK), drug metabolism (DM), bioanalysis (BA), LC, and MS (2–11).

The Role of Bioanalysis in Drug Discovery and Development

The development of new drugs is a complex, expensive, and multidisciplinary process. The modern drug development process often uses a molecular approach, which starts with an understanding of the biology and pathophysiology of the disease, the identification of the molecular target (a receptor or enzyme) responsible for the specific body malfunction, and the synthesis or discovery of a molecule (a small organic molecule or antibody) that binds to a physiological target, thereby mitigating a particular disease state (2). Because the drug must first be bound to the target to be effective, its distribution to the patient's systemic circulatory system is mandatory unless the drug can be delivered directly to the affected organ or target (3–6). Therefore, it is paramount to have accurate assessments of the drug concentrations in the patient's physiological fluids after administering the drug to the patient. For small-molecule drug products, oral dosage forms like tablets or capsules are generally preferred because of the ease in administering them: The patient ingests oral drug products to release the active pharmaceutical ingredient (API), which is then absorbed from the digestive system into the bloodstream to reach the intended target.

Bioanalysis is conducted during all new drug development phases—including initial research, drug discovery, preclinical, nonclinical, clinical development, and post-approval studies. Data from bioanalytical studies are collected to support various investigations, as can be seen in

TABLE I: Glossary of common terms, acronyms, and terminologies related to bioanalysis

Acronyms (Terms)	Full Names or Definitions
Bioanalysis Overview	
Pharmacology	Study of drug action—interactions of living organisms and exogenous chemicals that alter normal biochemical functions
PD, PK, DM, and BA	Pharmacodynamics (PD): What drugs do to the body or the relationship between drug concentration at the site of action and the effect on the body. Pharmacokinetics (PK): What the body does to the drugs or the study of the time course of drug absorption, distribution, metabolism, and excretion (ADME). Drug metabolism (DM): Biotransformation of drugs in the body. Bioanalysis (BA): Measurement of drugs and their metabolites in biological matrices.
Bioavailability, CL	The amount of drug absorbed vs. amount administered. Bioavailability is similar to drug exposure in some contexts. Clearance (CL): Rate of removal of a drug by various organs.
AUC, C_{max}, t_{max}, $t_{1/2}$	The area under the curve (AUC), maximum concentration (C_{max}), time to reach max concentration (t_{max}), the half-life of a drug in the body ($t_{1/2}$).
IVIVC	In vitro in vivo correlation (IVIVC); the correlation of in vitro data to in vivo results
PO, IV, IM, SC	Route of administration: peroral (oral) (PO), intravenous (IV), intramuscular (IM), subcutaneous (SC)
DS, DP, NCE, API	Drug substance (DS), drug product (DP), new chemical entity (NCE), active pharmaceutical ingredient (API)
Regulatory	
US FDA, EMA	US Food and Drug Administration, European Medicines Agency
IND, NDA, BLA	Investigational New Drug (IND), New Drug Application (NDA), Biologics License Application (BLA)
ICH	International Council of Harmonization. A consortium of regulators and pharmaceutical scientists that publish guidelines to expedite new drug development
GLP, GMP, GCP, GxP	Good Laboratory Practice (GLP), Good Manufacturing Practice (GMP), Good Clinical Practice (GCP). GxP is an acronym that collectively covers GLP, GMP, and GCP.
CMC	Chemistry, manufacturing, and controls
CoA	certificate of analysis (CoA).
QA, QC	Quality assurance (QA) is responsible for ensuring compliance with applicable quality management systems and regulations. Quality control (QC) is the laboratory branch of QA.
Liquid Chromatography, Mass Spectrometry	
HPLC, UHPLC	High-performance liquid chromatography (HPLC), Ultrahigh-pressure LC (UHPLC).
RPLC, HILIC	Modes of chromatography: Reversed-phase liquid chromatography (RPLC), Hydrophilic interaction liquid chromatography (HILIC).
SQ, TQ, IT, TOF, Orbital trap MS	Type of MS based on the analyzer: quadrupole (single quadrupole, triple quadrupole) (SQ, TQ), ion-trap (IT), time-of-flight (TOF), orbital trap MS.
ESI, APCI, TIC, SIM, MRM, SRM, PRM	Electrospray ionization (ESI), atmospheric pressure chemical ionization (APCI), total ion chromatogram (TIC), selected ion monitoring (SIM), multiple reaction monitoring (MRM), selected reaction monitoring (SRM), parallel reaction monitoring (PRM)

Table II. Readers seeking an in-depth understanding of these topics are encouraged to peruse the relevant references (4–6).

Fundamentals of High Performance Liquid Chromatography (HPLC) and MS in Bioanalysis

LC–MS is the primary analytical technique for the quantitative bioanalysis of small-molecule drugs in physiological fluids. This section describes LC–MS fundamentals and the rationales for selecting reversed-phase liquid chromatography (RPLC) with tandem mass spectrometry (MS/MS) detection as the predominant technique. The reader is referred to textbooks and review articles for details on HPLC (including RPLC (7,8), MS, and LC–MS (9–11). Table III lists the terminologies of HPLC and MS in bioanalysis and the advantages and limitations of RPLC with MS/MS detection.

RPLC is the predominant LC mode used in bioanalysis. The primary retention mechanism of RPLC is the hydrophobic interaction of the analytes with a bonded hydrophobic ligand (C18) to silica supports packed inside a column. Because the hydrophobic interaction force is weak, there is a reasonable assurance that all analytes in the sample will be eluted from the column with ~100% mass balance. RPLC is amenable to separating analytes with a wide polarity range under gradient conditions (7). Because most small-molecule drugs are basic (<80%), an acidic, aqueous mobile phase is generally used to keep the drug molecule in an ionized state which also suppresses the silanophilic activity of the bonded phases.

The key limitation of RPLC is the lack of retention for hydrophilic analytes that are better separated using a specialized RPLC bonded phase without end-capping or with a hydrophilic end-capping. A newer LC mode called *hydrophilic interaction liquid chromatography (HILIC)* has also been used successfully (7). In HILIC, one uses a hydrophilic stationary phase (such as silica) and a mobile phase similar to RPLC (acetonitrile and aqueous buffers). The analytes are eluted in an order that is opposite to that of RPLC, and the technique is less robust than RPLC. HILIC using MS-compatible mobile phases is particularly useful for analyzing secondary metabolites. Other HPLC modes, such as ion-exchange chromatography (IEC) and size-exclusion chromatography (SEC), are rarely used in bioanalysis because their mobile phases are generally not MS-compatible.

Triple-quadrupole mass spectrometry (TQMS) or MS/MS with electrospray ionization (ESI) and multiple or selected reaction monitoring (MRM

or SRM) is the primary technique used in bioanalysis because of its excellent reproducibility, sensitivity, specifically nanomolar (nM) or picomolar (pM) levels, and specificity (7,11). The impressive linear dynamic range (typically up to three or four orders of magnitude) allows the simultaneous quantitation of the API and lower-level metabolites in the same assay. A drawback of MS detection mode is the requirement of an internal standard for each analyte to compensate for loss during sample preparation, nebulization efficiency in the LC–MS interface, and the ion suppression and enhancement matrix effects (9–11). The internal standard used is preferably a stable isotopically labeled form of the analyte, which must be synthesized or purchased from a commercial vendor and added to the sample early during sample preparation.

Another limitation of MS is its inability to differentiate isobaric compounds. However, many diastereomers from multichiral NCEs can be separated by a well-developed HPLC method, and most enantiomer pairs can also be resolved using a chiral LC column (7). Ion mobility MS (IMS) is increasingly used to separate isomers based on differences in collisional cross-section. High resolution MS (HRMS) such as time-of-flight (TOF) and orbital trap MS, often available as hybrid (quadrupole time of flight, QTOF) instruments or "tribrid" (quadrupole–orbital ion trap) instruments, is a powerful tool for high-throughput screening applications or structure elucidation of metabolites (11,12). HRMS is invaluable in research to support particular investigations because it has a higher discrimination power to eliminate or reduce interferences from matrix components without MRM. Although they were not typically used in routine quantitative testing in the past, there has been an increasing trend recently in HRMS-based quantitation using new generations of HRMS instruments.

Workflow in Non-Regulated and Clinical Bioanalysis

On the laboratory side, the bioanalytical workflow is similar to most analytical testing procedures used in the quality assessment of drug substances and products (7). A key difference is the complex biological sample matrices, which require more sample cleanup, followed by a sensitive and selective quantitation of the API and its specified metabolites. Most bioanalytical studies are project-based, such as PK evaluation for initial NCE screening, good laboratory practice (GLP) toxicology studies, or testing patient samples under good clinical practice (GCP) regulations. The general workflow includes documented procedures such as sampling and sample preparation, method devel-

opment (calibration, LC–MS parameter optimization), method validation, sample analysis, and data processing and reporting (7,11). The final deliverables can include reports for initial PK studies, phase 1 dose-ranging for safety evaluation, or phase 4 bioequivalence studies to support new formulations. Reported data yield insights on drug absorption into the systemic circulation for bioavailability, the peak exposure of the drug (C_{max}), time taken for the maximum peak exposure (t_{max}), the half-life ($t_{1/2}$) for clearance of the drug in plasma, or the investigation of excretion and metabolic profiles, by measuring drug concentrations in plasma, urine, and feces for mass balance studies.

Regulatory Aspects of Bioanalysis

The development of regulations and guidelines is crucial to ensure ethical, controlled approaches to managing clinical trials and safeguarding the subjects. Efforts to provide regulatory guidance in bioanalysis started in 1990 with a global workshop in Crystal City, Virginia, which marked the beginning of a series of workshops known as "The Crystal City Bioanalytical Workshops" (13). These efforts led to the issuing of much useful regulatory guidance by the US FDA (14). However, it should be noted that this document provides "guidance," and is not a law or rule. Laboratory personnel should use their best judgment on a case-by-case basis as to the exact methodology for a given method and validation protocol.

Laboratories conducting bioanalytical studies generally operate under GLP guidelines, or Title 21 *Code of Federal Regulations* (*CFR*) Part 58 for nonclinical laboratory studies (15). In contrast, most manufacturing facilities operate under good manufacturing practice (GMP) regulations (16). Title 21 *CFR* Part 58 describes regulatory requirements for GLP facilities, equipment, testing operation, test and control articles, protocols, records, and reports. Other important guidance documents include the Organization for Economic Cooperation and Development (OECD) principles of GLP and consensus document (17), and the regulations on electronic records and signatures as described in 21 *CFR* Part 11 (18).

International Council for Harmonization (ICH) Guidelines

In an attempt to introduce international regulatory harmonization, a scientific consortium of regulators and pharmaceutical companies from Europe, Japan, and the United States created the ICH for Technical Requirements for Pharmaceuticals for Human Use. The focus of ICH is to improve the efficiency of new drug development, prevent duplication of clinical trials in humans, and minimize animal use while maintaining safeguards on quality, safety, efficacy, and regulatory obligations to protect public health. More information on ICH guidelines is available from www.ich.org. The ICH guideline for the validation of analytical procedure is particularly relevant to bioanalytical method validation (19).

Quality Management System (QMS)

At present, the pharmaceutical industry has proactively established a QMS in bioanalysis similar to that described in ICH guideline *Q10* (20) for manufacturing, which is focused on strategies and principles to ensure high-quality and consistent data. Some of the key components of the QMS supporting the regulated bioanalysis are listed here:

- *Test facility management and resources:* This includes the designated staff and facilities for the conduct of the study in a compliant manner.

TABLE II: Bioanalysis in various phases of new drug development

Research
• In silico and in vitro studies on plasma protein binding, metabolic stability, and plasma-blood distribution. • Animal studies to measure drug exposure, metabolism, clearance, and enzyme induction-inhibition. • Establishment and validation of pharmacological animal models to support drug candidate selection.
Drug Discovery and Preclinical
• Screening studies to build compound libraries, select leads, and optimize the structures of potential drug development candidates, including form and salt selection. A generic LC–MS method is generally sufficient for these preclinical screening studies. • Animal studies on exposure and response (PK/PD), absorption, distribution, metabolism, and elimination (ADME), bioavailability, dose-ranging finding, metabolite identification, tissue distribution, and pharmacological biomarkers. • IVIVC. The correlation of in vitro results with in vivo pharmacological effects in animal models. • Pivotal GLP toxicology studies in rodent and non-rodent species. Typically, this requires a validated LC–MS method.
Clinical: Clinical bioanalytical data are collected using validated methods to support regulatory filings. A validated bioanalytical method is required to measure drugs and relevant metabolites in blood, serum or plasma, target tissues, and urine.
• Phase 1: First-in-human safety evaluation in healthy subjects to support PK and dose-finding. • Phase 2: Proof-of-concept efficacy studies in patients. • Phase 3: Confirmation of dosing regimen and efficacy with final drug product in a large patient population. • Other studies: ADME assessment, drug–drug interaction, and mass balance studies. Biomarkers can be used to establish efficacy and clinical endpoints. IVIVC studies correlate in vitro release performance data with *in vivo* bioavailability to develop new oral dosages.
Post-Approval Studies:
• Therapeutic drug monitoring (TDM), pediatric studies, or studies to extend a drug product's applications to new indications. • Bioavailability (BA) and bioequivalence (BE) studies to support new or generic drug products.

- *Standard operating procedures (SOPs):* These are a set of instructions approved by management to ensure the quality and integrity of the data generated in bioanalysis.
- *Quality assurance program:* Test facilities have an independent quality assurance (QA) program to ensure data integrity and compliance with regulations for all programs.
- *Equipment and reagents:* Test facilities use validated equipment to generate, store, and retrieve the data. Likewise, the chemicals used in the study are documented with their respective identity, concentration, storage recommendations, stability, and expiration dating.
- *Sample handling and storage:* Samples are labeled to avoid any ambiguity in identification and stored in recommended conditions to ensure stability. A robust tracking system is in place to provide a chain of custody of all critical samples from receipt to disposal processes.
- *Laboratory information management system (LIMS):* Most laboratories supporting regulated bioanalysis use validated commercial or in-house developed software to oversee information regarding sample management, study protocols, assay development and validation, and analytical workflow to ensure data accuracy and integrity.
- *Clinical study–related aspects:* Patient safety, informed consent, and protecting the integrity of the study by installing proper measures to protect critical identification information in studies are the clinical study components that the bioanalytical testing site must also follow.

Modern Trends in Bioanalysis

Finally, we share our views on modern trends in bioanalysis relating to separation science technologies, sample collection and preparation, data analysis, and outsourcing and automation strategies adopted by many progressive pharmaceutical companies and contract research organizations (CROs).

HPLC

HPLC trends in bioanalysis are similar to other HPLC applications with the recent adoption of ultrahigh-pressure LC (UHPLC) and sub-2-µm columns to increase throughput and separation efficiency. Superficially porous particles (SPPs) are used to enhance column efficiencies (7) and HILIC for separating primary and secondary metabolites if RPLC does not retain them. Chiral LC is needed to separate enantiomers, although achiral RPLC methods are adequate for separating diastereomers for multichiral API. Faster autosamplers capable of injecting several samples per minute are used for high-throughput screening applications. Many LC–MS systems are multiplexed with parallel pumps and multi-samplers to increase sample throughput (7).

MS

MS/MS using TQMS with MRM or SRM detection remains the dominant preclinical and clinical testing technique. A wide linear dynamic range allows for simultaneous quantitation of the API and its metabolites. Modern TQMS instruments are becoming more compact and stackable with

reduced footprints and improved ion optics and ion transfer technology for increased sensitivity, dynamic, and mass range. Many modern chromatography data systems (CDS) are updated to perform data handling and MS control for the same manufacturers' TQMS systems (7).

HRMS using TOF, orbital trap MS, and hybrid MS are commonly used for metabolite identification and structure elucidation (7,12). HRMS is gaining popularity because it can generate more accurate quantitative data in preclinical screening studies to avoid severe interferences from endogenous components in the matrix.

IMS can separate molecules with the exact *m/z* ratios based on differences in shape or collisional cross-section. IMS is increasingly used to offer an additional dimension for the resolution of isobaric compounds without extensive HPLC method development effort for isomer separations (21).

TABLE III: Terminologies related to the use of HPLC and MS in bioanalysis

HPLC: RPLC (Reversed-phase Liquid Chromatography)
The primary retention mode of RPLC is the hydrophobic interaction of the analyte with the stationary phase (hydrophobic ligand [for example, C18]) bonded to silica supports. The mobile phase is a mixture of organic solvent and water. The aqueous mobile phase is generally acidified.
Advantages: RPLC has excellent reproducibility, separation power, and mass balance. It is amenable to analytes with a broad polarity range under gradient conditions.
TQMS: Triple Quadrupole MS (capable of performing MS/MS)
TQMS: In tandem quadrupole MS such as TQMS, the precursor ions are filtered in the first quadrupole, fragmented in the second quadrupole, followed by the quantitation of the signals from the selected product ions in the third quadrupole. The product ions are derived from the precursor ions, thus imparting selectivity, a prerequisite for complex matrices. Most clinical bioanalysis use TQMS with electrospray ionization (ESI) in MRM or SRM mode for accurate quantitation.
Advantages: MS/MS is a reproducible detection technique with very high sensitivity (nM or pM levels), specificity (or selectivity), and method linearity. It allows robust trace quantitation of multiple analytes in a complex matrix without elaborate sample preparation typically required for less selective detectors such as UV or single quadrupole LC–MS analyses.
Limitations: MS/MS typically employs an internal standard for each analyte to ensure accurate quantitation. Optimally, the internal standard is a stable isotope-labeled analog of the target molecule. The internal standard must be synthesized and is expensive to obtain. MS/MS is unable to separate signals from isobaric compounds coeluted with the exact *m/z* ratio. Matrix suppression (ionization suppression) is another major limitation if there is no adequate sample cleanup.

More Convenient and Efficient Sampling and Sample Preparation

Dried blood spot testing

The collection and transportation procedures for plasma or serum sample remains a labor-intensive and expensive process. The development of dried blood spot testing received much attention a decade ago for nonregulated and regulated bioanalysis (22,23). However, this testing has several bioanalytical challenges that need to be comprehensively addressed.

Patient-centric sampling (PCS)

PCS is a hot topic in the bioanalytical field. *PCS* constitutes new sample collection methods and technologies used in clinical trials where patients can follow instructions to self-collect samples and ship them to the testing facilities (24). Currently, there are multiple commercial vendors offering support in this direction.

Solid-Phase Extraction (SPE)

Microplates and Automation Devices

SPE microplates have improved the automated sample preparation platforms for bioanalysis in complex matrices (25). Innovations in new bonded phase and supports have reduced matrix interferences and allowed more sensitive and accurate assays for many problematic samples. New chemistries in SPE phases will be addressed in the next installment of this article series. Advances in automation devices that include liquid handling, aliquoting, filtration, and shaking using robotic arms or other platforms have significantly increased productivity in routine testing.

Data Analysis and Artificial Intelligence

Data analysis in bioanalysis is another workflow bottleneck that would benefit from more intelligent data systems and data integration platforms. Artificial intelligence (AI) in big data analysis has been shown to extract valuable clinical data with genetic testing in personalized medicine (26). These concepts and applications may soon expedite the correlation of pharmacological results with bioavailability, PK, drug–drug interaction, and other factors.

Outsourcing Trends

Bioanalytical outsourcing will continue to be a significant part of the regulated bioanalysis strategy of pharmaceutical companies globally. Sponsors are increasingly looking to outsource suitable development workloads to contract research organizations (CROs) for workforce bandwidth to manage additional drug development programs.

Summary and Conclusions

Bioanalysis of drugs in biological samples is a common LC–MS application performed by thousands of laboratories to support new drug development. It is challenging to generate accurate data of trace analytes in complex matrices in a stringent regulatory environment. In this article, we have strived to provide an overview of bioanalysis to the practicing scientist on LC–MS fundamentals, best practices, regulations, and modern trends of this challenging and rapidly evolving analytical methodology.

Acknowledgments

The author thanks the following colleagues for providing timely reviews and comments to improve the final manuscript's accuracy and clarity: Perry Wang and Jinhui Zhang at the US FDA; Naidong Weng at Janssen, J&J; Jack Henion, professor emeritus of Cornell University; Peng Yu at EpiQMax; and Eric Thomas, Stephanie Cape, and Mark Arnold at Covance.

References

(1) H. Hill, *Bioanalysis* **1**, 3–7 (2009). https://doi.org/10.4155/bio.09.3.

(2) R.G. Hill and H.P. Rang (Eds.), *Drug Discovery and Development: Technology in Transition* Churchill Livingston, Edinburgh, Scotland, 2nd ed., 2012).

(3) K. Whalen, *Lippincott Illustrated Reviews: Pharmacology* (Wolters Kluwer, New York, New York, 7th ed., 2018).

(4) H.S. Lee and K-H. Liu (Ed.), *Drug Metabolism, Pharmacokinetics and Bioanalysis* (Mdpi AG, Basel, Switzerland, 2019).

(5) S.H. Hansen and S. Pedersen-Bjergaard (Ed.), *Bioanalysis of Pharmaceuticals: Sample Preparation, Separation Techniques and Mass Spectrometry* (John Wiley & Sons, Hoboken, New Jersey, 2015).

(6) M.L. Rocci Jr. and S. Lowes, *Regulated Bioanalysis: Fundamentals and Practice* (Springer, Berlin, Germany, 2017).

(7) M.W. Dong, *HPLC and UHPLC for Practicing Scientists* (John Wiley & Sons, Hoboken, New Jersey, 2nd ed., 2019).

(8) M.W. Dong, *LCGC North Am.* **33**(10), 764–775 (2015).

(9) E. de Hoffmann and V. Stroobant, *Mass Spectrometry - Principles and Applications* (Wiley Interscience, Hoboken, New Jersey, 3rd ed., 2007).

(10) J.H. Gross, *Mass Spectrometry: A Textbook, 3rd Ed.* (Springer, New York, New York, 2017).

(11) W.A. Korfmacher, *Mass Spectrometry for Drug Discovery and Drug Development* (John Wiley & Sons, Hoboken, New Jersey, 2012).

(12) A. Kaufmann, *J. Mass Spec.* **55**, e4533 (2020). https://doi.org/10.1002/jms.4533.

(13) V.P. Shah and S. Bansal, *Bioanalysis* **3**(8), 823–827 (2011). https://doi.org/10.4155/bio.11.45.

(14) US Food and Drug Administration, *Bioanalytical Method Validation, Guidance for Industry* (FDA, Silver Spring, Maryland, 2018).

(15) *Code of Federal Regulations (CFR)*, Title 21, Parts 58 (U.S. Government Printing Office, Washington, D.C., 2011).

(16) *Code of Federal Regulations (CFR)*, Title 21, Part 211.194(a) (U.S. Government Printing Office, Washington, D.C., 2019).

(17) OECD, *Principles of Good Laboratory Practice, Environment Directorate* (Organization for Economic Co-operation and Development, Paris, France, 1998).

(18) *Code of Federal Regulations (CFR)*, Title 21, Parts 11 (U.S. Government Publishing Office, Washington, D.C., 2003).

(19) International Conference for Harmonization, *ICH Q2 (R1), Validation of Analytical Procedures: Methodology* (ICH, Geneva, Switzerland, November 1996, updated 2005).

(20) International Conference for Harmonization *ICH Q10, Pharmaceutical Quality System* (ICH, Geneva, Switzerland, 2009).

(21) M.W. Dong, *LCGC North Am.* **38**(4), 220–228 (2020).

(22) D.E. Raynie, *LCGC North Am.* **34**(11), 834–836 (2016).

(23) L. He, R. Gajee, R. Mangaraj, M. P. Waldron, and K.S. Brown, *Bioanalysis* **12**, 393–407 (2020). https://doi.org/10.4155/bio-2019-0180.

(24) D. Sentellas, J. Saurina, and O. Nunez, in *Handbooks in Separation Science* (Elsevier, Amsterdam, The Netherlands, 2020), pp. 673–698.

(25) K.P Bateman, *Bioanalysis* **12**, 971–976 (2020). https://doi.org/10.4155/bio-2020-0075.

(26) Research and Markets, *CISION PR Newswire, Lab Automation in Bioanalysis Markets, 2024 - Rising Demand for Personalized Medicines*. https://www.prnewswire.com/news-releases/lab-automation-in-bioanalysis-markets-2024-rising-demand-for-personalized-medicines--technological-innovations-resulting-in-improved-solutions-300872661.html.

ABOUT THE COLUMN EDITORS

Dr. Shashank Gorityala is a Senior Staff Scientist at Covance, in Madison, Wisconsin, where he supports bioanalytical method development.

David Roos is a Senior Scientist at Boehringer Ingelheim Pharmaceuticals, in Ridgefield, Connecticut,where he supports the development of regulated bioanalytical LC–MS methods for large and small molecules.

ABOUT THE AUTHOR

Michael W. Dong is a principal of MWD Consulting, which provides training and consulting services in HPLC and UHPLC, method improvement, pharmaceutical analysis, and drug quality. He was formerly a Senior Scientist at Genentech, a Research Fellow at Purdue Pharma, and a Senior Staff Scientist at Applied Biosystems/PerkinElmer. He holds a PhD in Analytical Chemistry from City University of New York. He has more than 130 publications and a best-selling book in chromatography. He is an editorial advisory board member of *LCGC North America* and the Chinese American Chromatography Association. Direct correspondence to: LCGCedit@mmhgroup.com.

FOCUS ON BIOPHARMACEUTICAL ANALYSIS

Tools for Functional Assessment of Biotherapeutics

Biologically derived therapeutics, such as monoclonal antibodies (mAbs), are playing an increasingly important role in revolutionizing modern medicine for treating cancer and many autoimmune disorders. They have significantly improved health care outcomes for patients because of their superior target specificity. Because the function of the drug is impacted via multiple pathways and perturbations at various levels of the protein architecture, a detailed study of functional assessment by using orthogonal tools has become a necessary part of their characterization. In the case of biosimilars, demonstration of biological comparability to the originator is an essential component of the comparability package that the manufacturer submits to the regulatory authorities. In this article, we present many of the various tools that are routinely used for performing such functional characterization of biotherapeutic products. Traditional cell-based approaches include measurement of the antibody-dependant cellular cytotoxicity (ADCC), complement-dependent cytotoxicity (CDC), and antibody-dependent cellular phagocytosis (ADCP). More recently, approaches based on ligand binding, including fluorescence-activated cell sorting (FACS), surface plasmon resonance (SPR), and biolayer interferometry (BLI) are commonly used as well. Current understanding of the role these approaches can play in a functional assessment has been elucidated.

Anurag S. Rathore, Rozaleen Dash, Ritu Jain, and Jared Auclair

Therapeutic biologics are becoming a critical and significant component of drug discovery pipelines in the pharmaceutical industry. The utility of biologic drugs for treating unmet medical needs is being expanded beyond oncology and immunology into other therapeutic areas, including cardiovascular and metabolic diseases (1). Drug disposition of biotherapeutics is vastly different from small molecules (2) and therefore, assessment of their safety and efficacy is critical for clinical development. Determining the safety of biotherapeutics often involves evaluating multiple factors, including those related to the product, patient, and treatment (3,4). Another trend is the rise of biosimilars, driven by the societal needs of affordable and accessible biotherapeutics. This has further necessitated the need for a meticulous and rigorous risk–benefit analysis of the biologics, involving establishing comparability of biosimilars. There are instances where process and formulation changes have been introduced to ensure similar quality, safety, and efficacy in line with the expectations, and a slew of guidelines have been issued by the regulatory authorities in this regard (2,5).

Several researchers have reported on development of platform methods or approaches for demonstrating analytical comparability with the reference product. Characterization of therapeutic monoclonal antibodies (mAbs) involves using a wide range of analytical techniques, along with ligand-binding and cell-based potency assays (6). Because publications on analytical comparability are commonplace, those on functional comparability are limited to determining either binding affinity to the receptors or the potency (depending on the mechanism of action) of the biosimilar on the relevant cell lines. Thus, considering the complexity of the therapeutic drug and the significant possibility that the function of the drug might be impacted via multiple pathways at various levels of the protein architecture, assessment of functional comparability is as important as analytical comparability.

Each functional assay has its pros and cons and hence just like in the case of analytical comparability, a platform of complementary assays is utilized. Table I summarizes the advantages and disadvantages of the most commonly used functional assays.

Design of bioassays for mAbs is driven by a physiological mechanism of action (MOA). Bioassays are always unique for each therapeutic, unlike other analytical techniques, and a well-designed functional assessment can precisely capture the biological activity of the mAb.

Ligand-Binding Assays (In Vitro Potency Assay)

Protein–protein interactions play a major role in the formation of protein complexes, which is the basis of various biological processes. The quantification of ligand binding to specific receptors is the key for drug development research, specifically for determining biological potency. The important aspects of ligand–receptor binding interactions include binding affinity and kinetics, thermodynamics, and ligand efficiency (7). Every step of ligand–target interactions can be studied by multiple binding assays.

Fluorescence-activated cell sorting (FACS) is the adopted method used to obtain a high purity sample of the product of interest. It allows purification of individual cells based on size, granularity, and fluorescence. It gives the percentage, actual number of cells, and mean fluorescence intensity (MFI) of the cell population, and can measure multiple parameters simultaneously on hundreds of individual cells per second; it is a powerful technology with a wide variety of applications in biopharmaceutics (8,9). Appropriate fluorochromes, dyes, conjugates, incubation temperatures, and periods are the essentials for cell surface protein estimation to get well-defined data from the samples.

Two prime tools that have gained prominence for establishment of functional comparability are surface plasmon resonance (SPR) and biolayer interferometry (BLI). Both techniques are optic-based label-free techniques that are used for estimating the biomolecular interaction profiles of biosimilar drugs. These two techniques are superior to traditional fluorescence or luminescence techniques, that are aided by labeling, because labeling is cumbersome and can occupy principal binding sites of the interacting molecule, thereby leading to conformational changes in the molecule and increase non-specificity in the analytical result (10,11).

SPR allows real-time, label-free detection of the interactions between biomolecules. Surface plasmon resonance is a phenomenon that occurs when polarized light strikes an electrically conducting surface at the interface of two media. This interaction generates plasmons, which are electron charge density waves, reducing the intensity of reflected light at a specific angle, referred to as the *resonance angle*. SPR is a powerful technique for measuring the binding of any pair of interacting molecules, including proteins, antibodies, and antigens. Interactions are measured in real-time, which enable the determination of kinetic parameters. The characterization of antibody–antigen interactions is essential for the successful development of biotherapeutics (9). For about two decades, SPR biosensors have been used to characterize antibody–antigen interactions with applications ranging from the low-resolution affinity screening of antibodies to the high-resolution kinetic constant determinations of the

Impurities Detection Simplified

The new LC 300 features both HPLC and UHPLC platforms and the new SimplicityChrom™ CDS software with a next-generation UI/UX design.

Kyle Oberndorfer
Chromatography
Portfolio Director
PerkinElmer

LCGC: How have you improved the analysis of impurities with the LC 300 and SimplicityChrom products?
OBERNDORFER: The analysis of impurities is a fundamental need that spans across almost every market and every industry. With the LC 300 and SimplicityChrom, we simplified the overall ownership and operating experience, making the system more friendly and responsive to customers' needs. The LC 300 is available as a UHPLC platform or as a high-performing HPLC platform. It features our new CDS software, SimplicityChrom, that controls the instrumentation fully and seamlessly while quickly and accurately collecting and processing large amounts of data.

Some labs only look at a few samples, but other labs may be looking at hundreds of samples, so we spent a lot of time focused on the overall productivity of the laboratory workflow—from the point the sample comes into the lab to the point a report or other output is provided to the end user, whether an internal or external customer.

LCGC: What shifts or advances in liquid chromatography have you adopted?
OBERNDORFER: If you rewind 15 years or so, it was the advent of UHPLC, which has been widely adopted within the pharmaceutical industry due to its shorter run times, solvent savings, and increased sensitivity. However, it hasn't been as widely adopted in many other markets or industries due to a combination of technical challenges, lack of applications development, and the perceived cost.

PerkinElmer has continued to build on the benefits of UHPLC's performance by focusing on simplification, robustness, ruggedized software control, and greater usability in our LC 300, which we think will open the door for UHPLC to enter more markets and more applications than before.

In addition to our 18,000 PSI UHPLC platform, we also have a high-performance HPLC system that can deliver up to 10,000 PSI. The platform allows users to stay with their traditional 1 ml/min-type LC applications but run more advanced column formats, such as superficially porous columns, that require a bit higher operating pressures but with UHPLC-like benefits including shorter runtimes, lower solvent usage and increased sensitivity.

LCGC: How has the importance of software design impacted the laboratory?
OBERNDORFER: One of the biggest impacts to lab productivity and throughput over the past 20 years has been advances in software, especially when you consider that up to 90% of the time while running HPLC is spent in front of a computer screen, controlling the instrument, and collecting and processing the data. The importance of software is disproportionately higher than the instrumentation itself.

SimplicityChrom really focuses on the entire user experience (UX)—it is intuitive and more workflow based—guiding you from sample introduction to reporting. We integrate both user interface (UI) (How does the screen look? Is it simplified? Is it easy for me to find things?) and UX (How are samples prepared and provided to you? How do you want or need to run your samples? How do you need or expect the results to be provided?) The science of UI and UX design is really taking the forefront in the digital revolution we're currently going through.

LCGC: What are some important but often overlooked functionalities when selecting an LC for the laboratory?
OBERNDORFER: When you look at and compare specifications, it is increasingly common not to see a lot of differences from vendor to vendor. However, it's important to spike out the overall UX because often there are capabilities and features that might seem subtle or nuanced but are really important in optimizing the total end to-end workflow of your lab.

For example, with our LC 300 system, we focused on giving the user a more simplified experience, meaning we've taken the complexity out of buying, owning, and maintaining the instrumentation. We integrated and built in previously separate modules, such as solvent degassing and a column oven, resulting in a much cleaner and simpler system. Now, you only have three LC modules in your stack that make it easier to maintain and operate. There is also the added benefit of reducing tubing volumes and tubing lengths, which chromatographers know is a good thing.

We also brought back a static color display that, at a glance, gives the user all of the instrument health parameters—pump pressure, flow rate, how stable the pressure is, what sample is currently in the queue, etc. This at-a-glance display eliminates going back and forth between the instrument and computer, which, throughout the course of a day, has a big impact on overall productivity. We opted for a static display instead of an interactive touchpad because any additional point-of-control or override on an instrument brings validation and compliance complexities.

We also added sample preparation capability into the autosampler, another huge time-saving feature. Often, a high percentage of time is spent doing sample preparation, e.g., diluting samples, adding an internal standard, creating calibrants, which can be done by the LC 300 Autosampler under full software control. Users can now incorporate standardization and traceability to their sample preparation, all while saving time. It's thinking beyond the instrument to the actual UX that really brings these benefits and productivity.

LCGC: It's interesting that PerkinElmer is bringing such an exciting product to the market. You have a strong reputation in many areas, but some might be surprised to learn of the long history and many advancements you have made in LC. Is that a fair observation?
OBERNDORFER: That is a fair observation. What's interesting is we do have a very long history in HPLC, and we're responsible for and proud of several significant innovations in the technology. As far back as the early 70s, PerkinElmer was in HPLC. We had a partnership with Nester-Faust, who we eventually acquired, and over the next 30 to 40 years, we had a lot of advancements. One of the first single-box LC systems in the early 80s was a PerkinElmer innovation, as was the advent of "Fast LC," where PerkinElmer pioneered small particles, 3-cm column lengths.

And our incorporation of the Nelson Analytical TurboChrom® CDS platform, which is now TotalChrom®, was one of the first enterprise chromatography data systems and was ever-present in many pharmaceutical and chemical laboratories in the 90s, bringing integrated data control, integrated compliance, and enhanced security.

We have a rich history in HPLC, and our involvement in the market has been targeted and focused in particular areas, but today we're asking, "How can we bring this collective history of great technology, renowned service, and support and make the larger industry aware of all that PerkinElmer has to offer in HPLC and UHPLC?"

TABLE I: The mechanism, advantages, and disadvantages of most commonly used biological assay methodologies

Assays	Mechanism	Advantages	Disadvantages
Ligand binding assays (in vitro potency assay)			
Fluorescence-activated cell sorting (FACS)	FACS allows purification of individual cells based on its size and granularity.	It estimates the cell surface protein affinity. It is preferred whenever very high purity of the desired population is demanded or when the target cell population expresses a very low level of the identifying marker.	It is sensitive to different fluorescence interferences. Also, the labeling of a ligand can lead to alterations in its binding characteristics.
Surface plasmon resonance (SPR)	SPR occurs when light-excited surface plasmon polaritons are used to track the binding of ligands to the receptors bound to a gold surface.	SPR is a rapidly emerging label-free ligand binding assay. It can be used to determine binding kinetics and affinity of the ligand.	This assay requires immobilization of one of the binding partners.
Biolayer interferometry (BLI)	BLI uses a spectrometer to detect interference patterns formed by light reflected from an optical layer and a biolayer containing protein of interest.	It is an effective approach to study binding kinetics.	This assay has been validated mostly for small molecule detection.
Cell-based potency assays (assessment of effector function)			
Antibody-dependant cellular cytotoxicity (ADCC)	It induces a cell-mediated immune defence whereby an effector cell of the immune system actively lyses a target cell, whose membrane-surface antigens have been bound by specific antibodies.	Data readout of this assay is driven by the target cell lysis endpoint. It is a high throughput assay for bulk antibody drug screening.	It is not convenient for standardization. Evaluation of several donors is required for accurate comparison and significant resources are required for cell preparation.
Complement-dependent cytotoxicity (CDC)	It induces a cascade of reactions of the immune system that kill pathogens by damaging their membranes.	Data readout for this assay is driven by the target cell lysis endpoint. It is a high throughput assay for bulk antibody drug screening.	It is not convenient for standardization. Significant resources are required for cell preparation. Error likely due to extensive manual operations.
Antibody-dependent cellular phagocytosis (ADCP)	It is a highly regulated process by which antibodies eliminate bound target molecules via connecting its fragment crystallizable (Fc) domain to specific receptor on phagocytic cells and bring out phagocytosis.	This assay is closely related to the true body immune microenvironment. It offers relatively low cost, high reproducibility, and a high success rate.	It is often neglected since the assay is extremely tedious.

antibodies, and the classification of antibody binding epitopes via epitope-binding studies (12).

BLI works on the principle of superimposition of electromagnetic waves of similar or different phases (13,14). BLI platforms comprise two interfaces, one between the glass fiber and the proprietary biomolecule, and the other between the surface chemistry and the solution. In addition, the BLI platform includes a disposable dip and an optical biosensor. Immobilization of a biomolecule on the surface tip of the glass fiber increases the pathlength of the reflection at the interface between surface chemistry and the solution that changes the interference patterns of all the wavelengths. When the interferometric profiles of the wavelengths are plotted, that results in a new profile that exhibits a shift to the right compared to the original profile. Therefore, if the immobilized molecule interacts with another molecule, there will be a further shift in the interferometric profile. This provides real-time kinetics and quantitation data of biomolecular interactions without the use of labeling (13,14).

Cell-Based Potency Assays

Although the ligand-binding assay can be performed readily with great precision and accuracy, the MOA typically involves post-ligand-binding and thus, the binding activity alone is an incomplete measure of potency. Evaluation of potency at the cellular level is required based on the understanding of the MOA for different targets. The biotherapeutic can typically either induce an early response (signalling pathway) or a late response (proliferation, cytokines).

MAbs target soluble receptors or cytokines on the cell surface and evaluation of this interaction can be achieved from cytotoxic assays including apoptosis to cell proliferation and metabolic assays. The anti-

gen-biding fragment (Fab) fragment of the mAb is mainly associated with binding specificity, while the antibody fragment crystallizable (Fc) portion is for the function of immunoglobulin G (IgG) at the cell level (15). There is significant discrepancy between the potency of mAb therapeutics measured in vitro and in vivo in regards to the required doses. Apart from complement activation, other effector functions are also important for MOA of mAbs.

As molecular-targeted biotherapeutics, antibodies that bind to specific cell-surface antigens on target cells can induce cytotoxicity via the effector functions of antibody-dependent cellular cytotoxicity (ADCC), complement-dependent cytotoxicity (CDC), and antibody-dependent cellular phagocytosis (ADCP) through the constant region of the Fc, and apoptosis of target cells (15,16). Establishment of an ADCC or CDC assay should be performed according to the characteristics of the mAbs because the assessment of effector functions is important for the development of the original mAbs candidates. Both in vitro assays are common tools for immunotherapeutic drug discovery and biosimilar development.

ADCC is a lytic mechanism that can be mediated by autoreactive IgG where monoclonal antibodies are able to elicit killing of antibody-coated target cells. The autoreactive IgG recruits effector cells to the target cells with the Fab portion of the IgG binding to the target cell and the Fc region associating with Fc receptors (FcR) on effector cells such as natural killer (NK) cells, monocytes, macrophages, neutrophils, eosinophils, and dendritic cells. Then, the Fc–FcR cross-linking results in the formation of an immune synapse leading to direct tumor cell lysis through the release of cytotoxic molecules (17).

CDC is a cytolytic cascade mediated by a series of complement proteins generously present in the serum. It is triggered by binding of complement component 1q (C1q) to the constant region of cell-bound antibody molecules (17,19). The first step of the complement cascade is binding of the C1q component to the Fc region, which affects the intensity of the following complement activations. A few approaches have succeeded in enhancing the CDC by facilitating the binding of the antibody constant region to the C1q component. As a result of the engineered amino acid mutations that have been inserted into either Fc or the hinge region, an improvement in C1q binding is observed (20).

The ADCP assay is based on using peripheral blood mononuclear cell (PBMC)-derived macrophages as effector cells. Monocytes are isolated from PBMCs and differentiated to macrophages in culture. The workflow is more sophisticated than ADCC and usually takes more than a week to retrieve macrophages. A dose-dependent curve is generated to assess the ADCP potency and phagocytosis is analyzed using flow cytometry. The ADCP assay is a powerful tool for the assessment of biocompatibility as well as early phage confirmation of in vivo (21–23).

Summary and Perspectives

Because of the complexity and intrinsic heterogeneity of mAbs, extensive physicochemical and biological characterization must be carefully conducted. In this article, we present the major tools that are used for functional characterization of mAb therapeutics, assessment methods and technologies that are used to characterize mAb-based candidate during preclinical and clinical studies. An important step in the successful development of a biosimilar is to establish robust analytical and functional comparability with the innovator (24). These are necessary for the biosimilar manufacturer to take advantage of the significant reduction in clinical data required for achieving regulatory approval (25). Functional tools have played an important role and have gradually emerged as a major resource for characterization of biosimilars, thereby playing a prime role in the biosimilar development. A comprehensive set of bioanalytical methods is typically used to analyze functional integrity and comparability (26, 27).

Establishment of cell-based potency assays is more useful than developing a ligand-binding assay because cell-based assays enable better detection of chemical modifications, such as deamidation in the complementarity-determining region or the Fc region of the molecule on its potency (28). Therefore, cell-based assays should be primarily chosen for product characterization, even for lot release, during the clinical development of mAb-based drug and post-licensure life-cycle management (29,30). However, cell-based methods are rather time-consuming and laborious and offer limited automation possibilities. Moreover, the detection format usually requires a label and a complex labelling protocol (9). The development of ligand-binding assays, used orthogonally, may prove to be a powerful and complementary tool in basic research, drug discovery and development, and downstream bioprocessing.

Competing Interests

No potential conflicts of interest were disclosed.

References

(1) A.S. Rathore, *Trends in Biotechnology* **27**, 698–705 (2009).

(2) M. Hassanein, M.A. Partridge, W. Shao, and A. Torri, *Bioanalysis* **12**(18), 1325–1336 (2020).

(3) A.M. Goetze, M.R. Schenauer, and G.C. Flynn, *mAbs* **2**(5), 500–507 (2010).

(4) A. Eon-Duval, H. Broly, and R. Gleixner, *Biotechnol. Prog.* **28**(3), 608–622 (2012).

(5) S.K. Singh, G. Narula, and A.S. Rathore, *Electrophoresis* **37**(17–18), 2338–2346 (2016).

(6) A.S. Rathore, I.S. Krull, and S. Joshi, *LCGC North Am.* **36**(11), 814–822 (2018).

(7) T. Aung, B. Chapuy, D. Vogel, D. Wenzel, M. Oppermann, M. Lahmann, T. Weinhage, K. Menck, T. Hupfeld, R. Koch, L. Trumper, and G.G. Wulf, *PNAS* **108**, 15336–15341 (2011).

• Continued on Page 284

Chromatography Fundamentals, Part X: Light Scattering Detection Systems for Size-Exclusion Chromatography

This contribution is a continuation of Part IX of this series. In that article, the fundamentals of light scattering as applied to SEC was introduced, including the origin and significance of pertinent equations related to the light scattering of macromolecules. In the present contribution, a summary of commercially available light scattering instrumentation is given, with emphasis on new detector technology. Owing to the complexity of data analysis and the many equations involved with light scattering measurements, a glossary of principal symbols and a table of relevant relationships are presented.

Howard G. Barth

This review is a continuation of Part IX (1), in which the theory of light scattering is given, including pertinent equations and data analysis. The following contribution is a summary of commercially available light scattering (LS) detection systems for size-exclusion chromatography (SEC). Information was obtained, for the most part, from current web sites and discussions with manufacturers, as of May, 2020. Please note that the author does not endorse any specific instrument.

In addition to detector sensitivity and noise specifications, selecting a light scattering instrument depends on many other factors, including software features and technical support. Furthermore, certain instruments now include dynamic light scattering capability for characterizing aggregates and particulates, which will be the subject of Part XI of this series.

Light scattering detectors for SEC are currently available from Agilent Technologies, Brookhaven Instruments, Malvern Panalytical, Postnova Analytics, Tosoh Bioscience, and Wyatt Technology Corporation. The low-angle capabilities of Malvern's low angle light scattering/right angle light scattering (LALS/RALS) (7°/90°) and Agilent's dual-angle detector (15°/90°) use collimated annulus optics for low-angle measurements and photodiodes for right-angle detection. Moreover, Agilent's instrument utilizes fiber optics to transmit scattering signals to the sensor. Other mutiangle instruments employ an array of photodiodes that surround the flow cell, placed at specified angles for detecting scattered light, with the exception of Brookhaven Instruments that employs a charge-coupled device (CCD) for detection.

The apparent trend among some companies is to maximize the number detection angles for improved accuracy and precision. For example, Wyatt Technology, Malvern Panalytical, and Postnova Analytics sell instruments that have 18, 20, and 21 angles of measurement, respectively.

For most instruments, the low-molecular-weight limit ranges from about 200 to 10^3 g/mol. By reason of equation 7c from Part IX, the lower limit can be adjusted by increasing injection concentration. It is important to note, that when measuring the low-molecular tail of a polydisperse sample, realistic molecular-weight detection limits greatly exceed the above range. The lower radius-of-gyration limit appears to be about 10 nm, except, for example, Tosoh Bioscience LenS3 (see following section) and Postnova multiple angle light scattering (MALS) detectors, whose lower limits are approximately 5 and 8 nm, respectively, using typical injection concentrations. Here the lower limit of angular dissymmetry depends primarily on the sensitivity and signal/noise of the instrument.

It should be stressed that lower molecular-weight and radius-of-gyration limits depend, among other attributes, on instrument design, intensity and wavelength of the incident beam, scattering volume, and photocell sensitivity. Specifications are also based on such factors as the specific refractive index of the sample, injection amount, signal-to-noise ratio of the light scattering and concentration detectors, baseline drift, peak broadening from columns and detector cell volume, and other chromatographic conditions.

It is of interest to note that a radius-of-gyration limit of 10 nm corresponds to 10^5 g/mol for linear, random-chain polymers. For polymers that are smaller than 10 nm, viscometric detectors can be used, provided that universal calibration is valid, a topic that will be covered in Part XII of this series.

New MALS Detector Technology

Tosoh Bioscience has recently introduced a mutiangle instrument (LenS3 MALS) that is capable of measuring radii of gyration well below 10 nm and molecular weights less than 500 using typical injection concentrations. This newly designed instrument has a conically shaped flow cell (referred to as a chamber), composed of blackened poly(ether ketone) to absorb stray scattered light. It also is equipped with a green laser-diode (505 nm), rather than longer wavelength diodes (635 to 680 nm), typical in some other detectors, with the exception, for example, of Postnova Analytics's 532-nm light source. Because of the 4th-power dependency on wavelength, the intensity of scattered light at 505 nm, as compared to 635–680 nm, is increased by a factor of 2.3–3.0, representing a significant increase in sensitivity.

The cell design and optical pathway of the LenS3 MALS instrument are illustrated in Figures 5 and 6, respectively. (Figure designations are continued from Part

If your standards and your samples are the same size, they must be the same mass, right?

With DAWN you can determine absolute molecular weights and sizes without using reference standards made in someone else's lab.

That's the problem with calibration-based measuring techniques. You don't know—you can only assume. Which is why every major pharmaceutical and biotechnology company, as well as most federal regulatory agencies are switching from relative methods to Wyatt Technology's absolute measurements. Our DAWN® multi-angle light scattering (MALS) instruments allow you to determine absolute molecular weights and sizes without relying on so-called standards, or measurements made in someone else's lab. Wyatt instruments measure all of the quantities required for determining absolute molar masses directly.

Learn how to end you dependence on reference standards forever at wyatt.com/NoRef

WYATT TECHNOLOGY
wyatt.com

TABLE I: SEC-LS of styrene oligomers of a polystyrene standard A-500 (Tosoh Bioscience) measured at 10^0 using the detector and GPC system as described in the *New MALS Detector Technology* section. Chromatographic conditions: DRI at 35 °C; mobile phase: THF; injection volume: 50 µL; injected concentration: 8.54 mg/mL; flow rate: 1 mL/min; column set: TSKgel G3000HXL, G2500HXL, G2000HXL (7.8 mm ID x 300 mm for each column).

Degree of Polymerization	Predicted MW[1]	Measured M_p[2]	Error[3], %
2	266	260	−2.2
3	370	380	+2.7
4	474	500	+5.4
5	587	620	+5.6
6	682	720	+5.6
7	786	850	+8.1
8	890	990	+11.2
9	994	1100	+10.7

[1]MW includes 58 g/mol attributed to end groups.
[2]Molecular weight at peak maximum.
[3]Systematic errors might have been attributed to the fact that the same specific refractive index, 0.170 mL/g, was applied to all oligomers.
Source: Adapted from data courtesy of Tosoh Bioscience.

TABLE II: SEC-LS of narrow molecular-weight-distribution polystyrene standards measured at 10°, 90°, and 170° using the detector and GPC system as described in the *New MALS Detector Technology* section. Chromatographic conditions: DRI at 40 °C; mobile phase: THF; injection volume: 80 µL; flow rate: 1 mL/min; column set: two TSKgel GMH_{HR}-N columns (7.8 mm ID x 300 mm); column temperature: 40 °C (Data courtesy of Tosoh Bioscience)

Sample[1] Code	Injected Conc., mg/mL	Measured[2] M_p	Literature Value[3], R_g, nm	Measured R_g, nm	Diff., %
A5000	4.81	5,800	2.04	2.1	+2.9
F-1	4.27	10,600	2.93	3.0	+2.4
F-2	3.22	18,600	4.32	4.3	-0.5
F-4	2.79	40,500	6.69	6.6	-1.3
F-10	1.97	100,000	N/A	10.5	NA
F-20	1.02	196,000	16.2[4]	15.8	-2.5

[1]Polystyrene standards from Tosoh Bioscience.
[2]Peak-maximum molecular weight.
[3]Determined from small-angle x-ray scattering in toluene at 15.0 °C (2).
[4]Extrapolated value by Tosoh Bioscience.
Source: Adapted from data courtesy of Tosoh Bioscience.

TABLE III: Glossary of principal symbols used in this article and Part IX (1).

Symbol	Definition
A_2	Second virial coefficient
dn/dc	Specific refractive index or increment of a polymer in solution.
c	Polymer concentration
g	Branching index
i_s'	Scattered light intensity of a single particle in vacuo.
$i_{s,p}$	Scattering intensity of a polymer in solution.
I_o	Scattering intensity of the incident light.
I_θ	Scattering intensity at angle θ
k	Arbitrary constant used to spread out data of Zimm plot.
K	Optical constant

Continued on Page 282

IX.) Eluent enters from the bottom of the flow chamber, splits into two pathways, which are then combined before exiting. For increased sensitivity, the unit is constructed such that nearly the entire cell volume or path length acts as the scattering volume. This is accomplished by passing the incident beam through the center of the cell, allowing forward scattering to be measured at 10° (low-angle LS or LALS) and back scattering at 170° (high-angle LS or HALS); these supplementary angles are close to the theoretical limits of 0° and 180°, contributing to greater radius-of-gyration sensitivity. In addition, scattered light intensity is also measured at 90° (right-angle LS or RALS).

The high sensitivity and low baseline noise are demonstrated by the analysis of a mixture of styrene oligomers in tetrahydrofuran, ranging from dimer to nonamer. These data, given in Table I, show that the instrument is capable of measuring the molecular weight of styrene oligomers, as low as 260 g/mol for the dimer with an error of −2% when compared to the predicted value. Note that the same specific refractive index, 0.170 mL/g, was applied to all oligomers, which may have contributed to the progressively increasing error. The total mass of sample injected was only 0.43 mg of which approximately 30 µg was attributed to the dimer.

The LenS3 MALS instrument uses angular dissymmetry, rather than Zimm's method, to calculate the radius of gyration. With this approach, the particle scattering function is represented as a ratio of scattering intensities,

$$P_\theta = I_\theta / I_{0^\circ} \qquad [22]$$

in which I_{0° is the scattering intensity taken at 10°. Furthermore, an instrument normalization factor, N_θ, is employed that corrects for scattering volume, detector sensitivities, and distances from the scattering volume to the detector. Thus, for each elution volume increment, three particle scattering functions are generated:

$$P_{0^\circ} = (I_{0^\circ} / I_{10^\circ})\, N_{0^\circ} = 1 \qquad [23a]$$

$$P_{90^\circ} = (I_{90^\circ} / I_{10^\circ})\, N_{90^\circ} \qquad [23b]$$

Increased Sensitivity with the LenS3® MALS Detector!

Don't have a LenS3 MALS yet? See what you are missing:
Quantifiable Results at Low Concentrations!

Analysis of Rituximab, MW ~150,000 Da on UHPLC using TSKgel® UP-SW2000, 2 µm, 4.6 mm ID × 30 cm column with LenS3 MALS and competitive MALS system

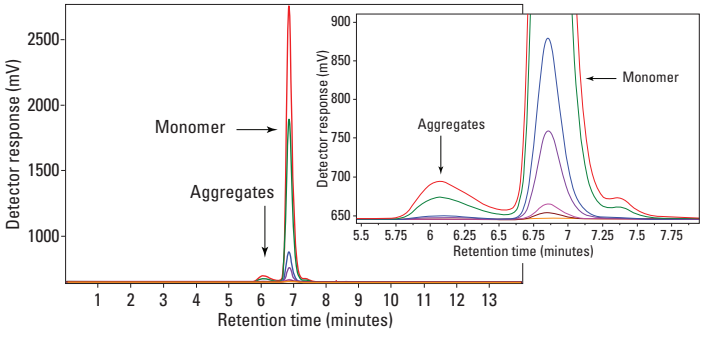

LenS3 MALS Detector

#	Concentration (mg/mL)	Load (µg)	SN Monomer	Injection volume (10 µL) Monomer -MW	Injection volume (10 µL) Aggregate -MW
1	1	10	8000	150800	276600
2	0.5	5	5000	150400	285000
3	0.1	1	800	153000	253300
4	0.05	0.5	400	152300	250600
5	0.01	0.1	80	154500	-
6	0.005	0.05	40	153600	-
7	0.001	0.01	10	160800	-

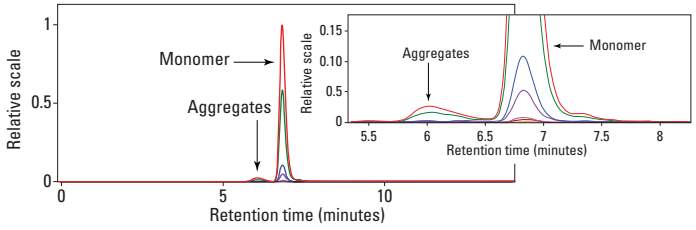

Competitive MALS Detector

#	Concentration (mg/mL)	Load (µg)	SN Monomer	Injection volume (10 µL) Monomer -MW	Injection volume (10 µL) Aggregate -MW
1	1	10	530	135200	276400
2	0.5	5	310	135900	262000
3	0.1	1	60	137400	819000
4	0.05	0.5	20	137900	949600
5	0.01	0.1	5	108900	-
6	0.005	0.05	2	107500	-
7	0.001	0.01	-	-	-

Competitive separations may not be representative of all applications.

LenS3 delivers:

- **better quality of data with more accurate and precise results when compared to standard detectors.**
- **improved signal to noise, allowing lower LOD and LOQ as well as 15x more sensitivity at 10 µg nominal loading!**

LenS3 is the first choice when analyzing proteins, aggregates and other impurities for reliable MW determinations across multiple load levels.

TOSOH BIOSCIENCE
www.tosohbioscience.com

TOSOH

TABLE III (CONTINUED): Glossary of principal symbols used in this article and Part IX (1).

Symbol	Definition
M	Molecular weight
M_n	Number-average molecular weight
M_w	Weight-average molecular weight
M_z	z-average molecular weight
n_o	Refractive index of the solvent or mobile phase, used in place of the polymer solution.
N_A	Avogadro's number
N_θ	Instrument normalization factor
$P(\theta)$ or P_θ	Particle scattering function
r	Radial distance from scattering volume to the detector.
R_g^2	Mean-square radius of gyration of a polymer molecule.
R_g	Root-mean-square radius of gyration, commonly shortened to radius of gyration.
$R_{g,n}$	Number-average radius of gyration
$R_{g,w}$	Weight-average radius of gyration
$R_{g,z}$	z-average radius of gyration
$R_{\theta,soln}$	Rayleigh ratio of polymer solution.
$R_{\theta,solv}$	Rayleigh ratio of solvent.
$\bar{R}_\theta$	Excess Rayleigh ratio
V	Scattering volume
α	Molecular polarizability
θ	Scattering angle
λ	Wavelength of light within solvent or polymer solution, equal to λ_o/n_o.
λ_o	Wavelength of the incident light in vacuo.
μ_θ^2	Angular parameter

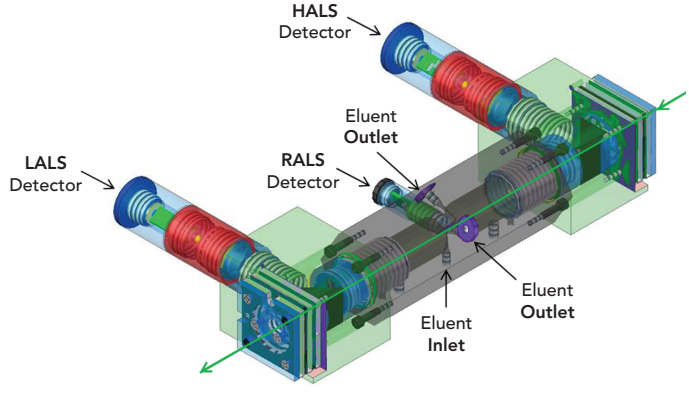

Source: Courtesy of Tosoh Bioscience.

FIGURE 5 (NOTE: Figure numbers are continued from Part IX): Configuration of a newly designed SEC/multiangle instrument using the detector and GPC system as described in the *New MALS Detector Technology* section. This model is capable of measuring radii of gyration as low as 2 nm and molecular weights less than 500 g/mol using typical injection concentrations. Eluent enters from the bottom of a conically shaped flow chamber from two inlets, which are then combined before exiting the cell. The three photodiodes measure scattered light intensities at low (10°, LALS), high (170°, HALS) and right angles (90°, RALS).

$$P_{170°} = (I_{170°}/I_{10°})\, N_{170°} \qquad [23c]$$

With this procedure, the particle scattering function (equation 9) is expressed as,

$$\lim_{\theta\to 0} P(\theta) = 1 - [(16\,\pi^2 R_g^2)/(3\lambda^2)]\sin^2(\theta/2) \qquad [24]$$

By using an angular parameter,

$$\mu_\theta^2 = (4\pi/\lambda)^2 \sin^2(\theta/2) \qquad [25]$$

equation 24 now becomes

$$\lim_{\theta\to 0} P(\theta) = 1 - \mu_\theta^2\,(R_g^2/3) \qquad [26a]$$

which is referred to as the Guinier relationship (15). Since $P_\theta = I_\theta / I_{0°}$, equation 26a becomes

$$I_\theta / I_{0°} = 1 - \mu_\theta^2\,(R_g^2/3) \qquad [26b]$$

By plotting $I_\theta/I_{0°}$ against μ_θ^2, the y-intercept is $P_{0°} = (I_{0°}/I_{10°})N_{0°} = 1$, and the initial slope (at the intercept) is $-R_g^2/3$.

An example of this angular dissymmetry approach is given in Figure 7, in which a broad polystyrene standard (NIST SRM 706a) was analyzed by the LenS3 MALS detector, courtesy of Tosoh Bioscience. Owing to a slight amount of curvature, a quadratic equation ($P_\theta = 1 - b\mu_\theta^2 + c\mu_\theta^4$) was used to fit the data, which gave $R_{g,z}$ = 27 nm, in agreement with the literature value. Owing to the low noise level and high sensitivity of the instrument, only three angles are required for radius-of-gyration and molecular weight measurements.

Table II shows preliminary molecular weight and radius-of-gyration data of a series of nearly monodisperse polystyrene standards, adapted from data supplied by Tosoh Bioscience. Radii of gyration were in agreement with literature data obtained from small-angle x-ray scattering, whose authors used similar lots of polystyrene standards dissolved in toluene (2). These initial results were well below the established limit of 10 nm. As previously noted, detection limits depend upon many factors that can contribute to the signal-to-noise ratio (S/N) of both the light scattering instrument and concentration detector, such as baseline noise and drift, column effi-

ciency, injection amount, and specific refractive index of the sample.

Conclusions

Light scattering is the ideal detector for SEC, because it provides molecular weight and radius-of-gyration distributions in addition to corresponding statistical averages without column calibration. With this detector, the only information that is required is the specific refractive index of the polymer and the refractive index of the mobile phase.

By using low injection concentrations, the Rayleigh equation is reduced from three (M, R_g, and A_2) to two unknowns (M and R_g), greatly facilitating data analysis. Moreover, if low-angle measurements are used, molecular weight can be determined directly without resorting to graphical analysis, however, molecular size information is lost.

To increase the reliability of molecular weight and radius-of-gyration measurements, several instrument companies have opted to maximize the number of photodiodes that surround the flow cell; for example, Wyatt Technology, Malvern Panalytical, and Postnova Analytics have instruments of 18, 20, and 21 angles, respectively. Of late, Postnova Analytics and Tosoh Bioscience have instruments with green- rather than red-laser diodes, resulting in increased sensitivity. Furthermore, Tosoh Bioscience's instrument consists of a newly designed flow cell and optical system that can measure the radii of gyration as low as about 2 nm under ideal condition. With normal injection amounts, the radius-of-gyration limit is approximately 5 nm, and the molecular weight limit is below 500 g/mol for polystyrene.

For the reader's benefit, a glossary of principal symbols and a summary of relevant equations and their significance are given, respectively, in Tables III and IV.

Parts XI and XII of "Chromatography Fundamentals" will be devoted to online dynamic light scattering and viscometric detectors, respectively.

Acknowledgments

The author gratefully acknowledges Cara Tomasek, David Gillespie, and Sébastien Rouzeau, all from Tosoh Bio-

TABLE IV: Summary of important light scattering relationships in Parts IX and X. The most useful equations are highlighted in red. (SI: scattering intensity; LS: light scattering)

No.	Equation	Description
1	$i_s = 16\pi^4 (I_o/r^2)(\alpha^2/\lambda_0^4)$	SI of a single particle in vacuo
2	$i_{s,p}\, r^2/VI_o = 16\pi^4 (\alpha^2/\lambda^4)(N_A c/M)$	Normalized SI of polymer in solution
3	$\alpha^2 = [M^2/(4\pi^2 N_A^2)]\, n_0^2 (dn/dc)^2$	Molecular polarizability, responsible for LS signal
4	$i_{s,p} r^2/I_0 V = (4\pi^2/\lambda^4)(Mc/N_A) n_0^2 (dn/dc)^2$	Eqn 3 substituted into 2.
5	$K=(4\pi^2 n_0^2/N_A^4)(dn/dc)^2$	Optical constant: consists of terms needed prior to LS analysis.
6	$i_{s,p}\, r^2/(I_0 V) = KMc$	Eqn 5 substituted into 2.
7a	$i_{s,p}\, r^2/(I_0 V) = i_{s,soln}\, r^2/I_0 V - i_{s,solv}\, r^2/I_0 V$	Experimentally determined, normalized SI of polymer in solution.
7b	$\bar{R}_\theta = R_{\theta,soln} - R_{\theta,solv}$	Eqn 7a changed to LS notation.
7c	$\bar{R}_\theta = KMc$	Uncorrected excess Rayleigh ratio for LALS data analysis.
8a	$\bar{R}_\theta = K\,[c/([MP(\theta)]^{-1} + 2A_2 c)]$	Eqn 7c corrected for nonideal behavior.
8b	$Kc/\bar{R}_\theta = [MP(\theta)]^{-1} + 2A_2 c$	Standard form of eqn 8a
9	$\lim_{\theta\to 0} P(\theta)^{-1} = 1 + [(16\pi^2 R_g^2)/(3\lambda^2)] \sin^2(\theta/2)$	Particle scattering function
10	$Kc/\bar{R}_\theta = 1/M + [R_g^2 (16\pi^2)/(3\lambda^2 M)] \sin^2(\theta/2) + 2A_2 c$	Eqn 9 substituted into eqn 8b for MALS data analysis.
11a	$\lim_{\substack{\theta\to 0 \\ c\to 0}}$ intercept $= 1/M$	MALS y-intercept
12a	$\lim_{\theta\to 0}$ slope $= R_g^2\, [16\pi^2/(3\lambda^2 M)]$	MALS angle-dependent slope
13	$\lim_{c\to 0}$ slope $= 2A_2$	MALS concentration-dependent slope
21a	$Kc/\bar{R}_\theta = 1/M$	Standard form of eqn 7c
22	$P_\theta = I_\theta/I_{0^\circ}$	y-axis of angular dissymmetry plot
24	$\lim_{\theta\to 0} P(\theta) = 1 - [(16\pi^2 R_g^2)/(3\lambda^2)] \sin^2(\theta/2)$	Reciprocal of $\lim_{\theta\to 0} P(\theta)^{-1}$ (eqn 9) for angular dissymmetry plot.
25	$\mu_\theta^2 = (4\pi/\lambda)^2 \sin^2(\theta/2)$	x-axis of angular dissymmetry plot
26	$\lim_{\theta\to 0} P(\theta) = I_\theta/I_{0^\circ} = 1 - \mu_0^2 (R_g^2/3)$	Eqn 25 substituted into 24: angular dissymmetry or Guinier relationship.

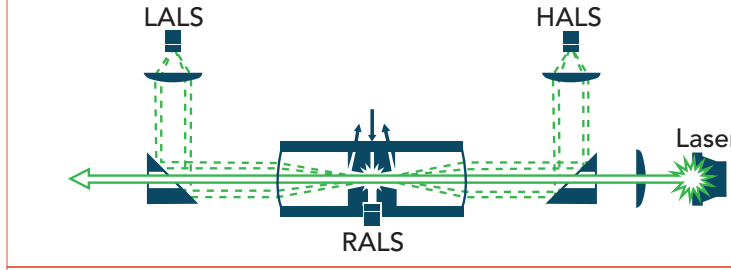

Source: Courtesy of Tosoh Bioscience.

FIGURE 6: Schematic of the optical pathway of a highly sensitive SEC/multiangle instrument. The incident beam of a 505-nm laser diode passes through the center of the cell, allowing forward scattering to be measured at 10° (low-angle LS or LALS), back scattering at 170° (high-angle LS or HALS), as well as at 90° (right-angle LS or RALS). The low-wavelength light source, long optical pathway, and widely spaced supplementary scattering angles contribute to the high sensitivity of the detector.

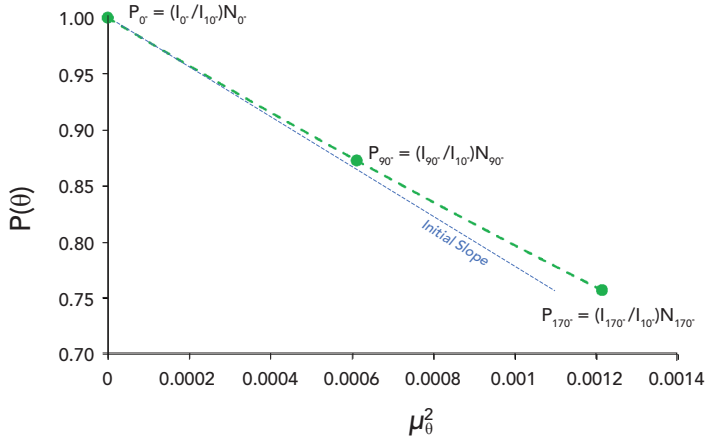

Source: Courtesy of Tosoh Bioscience.

FIGURE 7: Angular dissymmetry plot of a broad polystyrene standard (NIST SRM 706a) analyzed by SEC/light scattering using the detector and GPC system as described in the *New MALS Detector Technology* section. The particle scattering function, P_θ, measured at 10°, 90°, and 170° is plotted against the angular parameter, μ_θ^2, where $P_{0°} = I_{10°}N_\theta$, I_θ is the scattering intensity at angle θ, N_θ is a normalization factor, and $\mu_\theta^2 = (4\pi/\lambda)^2\sin^2(\theta/2)$. A quadratic equation was used to fit the data, in which $R_{g,z}$ = 27 nm.

science, for their insightful discussions on light scattering and for providing figures and preliminary data on the LenS3 MALS instrument.

LenS is a registered trademark of Tosoh Bioscience LLC.

EcoSEC and TSKgel are registered trademarks of Tosoh Corporation.

References

(1) H.G. Barth, *LCGC North Am.* **38**(10), 569–579 (2020).

(2) F. Abe, Y. Fumiaki, T. Yoshizaki, and H. Yamakawa, Macromolecules, **26**(8), 1884–1890 (1994).

Howard G. Barth is with Analytical Chemistry Consultants, Ltd., in Wilmington, Delaware. Direct correspondence to: howardbarth@gmail.com.

• Continued from Page 277

(8) I. Jilani, S. O'Brien, T. Manshuri, D.A. Thomas, V.A. Thomazy, M. Imam, S. Naeem, S. Verstovsek, H. Kantarjian, F. Giles, M. Keating, and M. Albitar, *Blood* **102**(10), 3514–3520 (2003).

(9) M. Cedeño-Arias, J. Sanchez-Ramirez, R. Blanco-Santana, and E. Rengifo-Calzado, *Sci Pharm.* **79**(3), 569–581 (2011).

(10) D. Frenzel and D. Willbold, *PLoS One* **9**(9), e106882 (2014).

(11) A.S. Rathore, I. Krull, J. Batra, and D. Kumar, *LCGC North Am.* **35**(12), 870–877 (2017).

(12) A.S. Rathore and R. Dash, *BioPharm Int.* **32** (3), 34–39 (2019).

(13) X.R. Jiang, A. Song, S. Bergelson, T. Arroll, B. Parekh, K. May, S. Chung, R. Strouse, A. Mire-Sluis, and M. Schenerman. *Nat Rev Drug Discov.* **10**, 101–110 (2011).

(14) P. Hariharan, *Basics of Interferometry* (Academic Press, Massachusetts, 2007), pp. 3–5.

(15) R. Barbour and M.P. Bova, *Bioanalysis* **4**, 619–622 (2012).

(16) X. Wang, Z. An, W. Luo, N. Xia, and Q. Zhao, *Protein Cell* **9**(1), 74–85 (2018).

(17) M. Tada, A Ishii-Watabe, T. Suzuki, and N. Kawasaki, *PLoS One* **9**(4), e95787 (2014).

(18) N. Nupur, N. Chhabra, R. Dash, and A.S. Rathore, *mAbs.* **10**(1), 143–158 (2018).

(19) S. Lida, R. Kuni-Kamochi, K. Mori, H. Misaka, M. Inoue, A. Okazaki, K. Shitara, and M. Satoh, *BMC Cancer* **9**, 58 (2009).

(20) S. Lida, H. Misaka, M. Inoue, M. Shibata, R. Nakano, N. Yamane-Ohnuki, M. Wakitani, K. Yano, K. Shitara, and M. Satoh, *Clin. Cancer Res.* **12**, 2879–2887 (2006).

(21) A.W. Pawluczkowycz, F.J. Beurskens, P.V. Beum, M.A. Lindorfer, J.G.J van de Winkel, P.W.H.I. Parren, and R.P. Taylor, *J. Immunol Methods* **183**(1), 749–758 (2009).

(22) N. Gül and M.V. Egmond, *Cancer Res.* **75**(23), 5008–5013 (2015).

(23) L. Kamen, S. Myneni, C. Langsdorf, E. Kho, B. Ordonia, T. Thakurta, K. Zheng, A. Song, and S. Chung, *J. Immunol Methods* **468**, 55–60 (2019).

(24) A. Ishii-Watabe and T. Kuwabara, *Drug Metab Pharmacokinet.* **34**(1): 64-70 (2019).

(25) E.R. Kabir, S.S. Moreino, and M.K.S. Siam, *Biomolecules* **9**(9), 410 (2019).

(26) A.S. Tsiftsoglou, S. Ruiz, and C.K. Schneider, *BioDrugs* **27**(3), 203–211 (2013).

(27) H. Schellekens, *Nat Biotechnol.* **22**(11), 1357–1359 (2004).

(28) A.S. Rathore, *Biomarker Discovery in the Developing World: Dissecting the Pipeline for Meeting the Challenges* (Springer, New Delhi, 2016).

(29) T.T. Hansel, H. Kropshofer, T. Singer, J.A. Mitchell, and A.J.T. George, *Nat. Rev. Drug Discov.* **9**, 325–338 (2010).

(30) R. Bansal, R. Dash, and A.S. Rathore, *J. Pharm. Sci.* **109**(9), 2684–2698 (2020).

ABOUT THE CO-AUTHORS

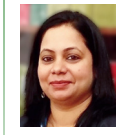

Rozaleen Dash is with the Department of Chemical Engineering at the Indian Institute of Technology in Delhi, India.

Ritu Jain is with the Department of Chemical Engineering at the Indian Institute of Technology in Delhi, India.

ABOUT THE COLUMN EDITORS

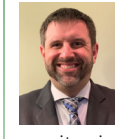

Jared Auclair is an Associate Dean of Professional Programs and Graduate Affairs at the College of Science at Northeastern University, in Boston, Massachusetts. He is also the Director of Biotechnology and Informatics, as well as the Director of the Biopharmaceutical Analysis Training Laboratory.

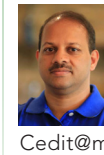

Anurag S. Rathore is a professor in the Department of Chemical Engineering at the Indian Institute of Technology in Delhi, India. Direct correspondence to: LCGCedit@mmhgroup.com

SUPPLEMENT TO
LC GC north america
solutions for separation scientists

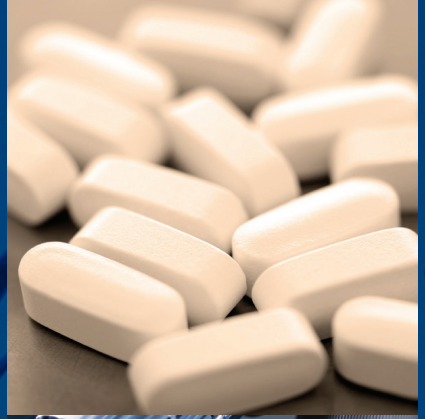

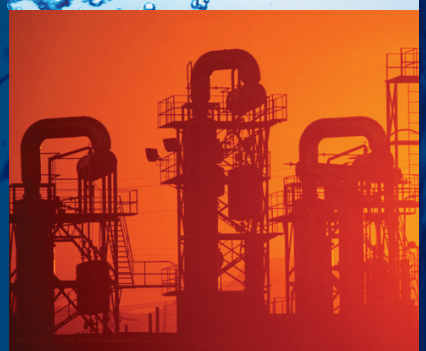

THE APPLICATION NOTEBOOK

June 2021
www.chromatographyonline.com

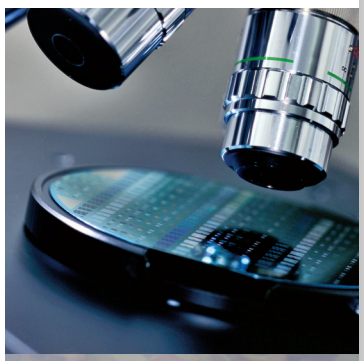

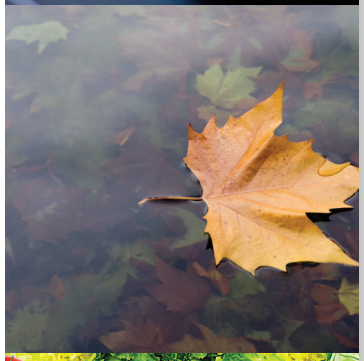

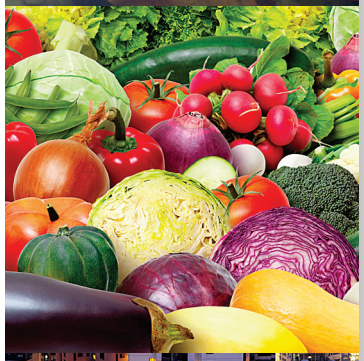

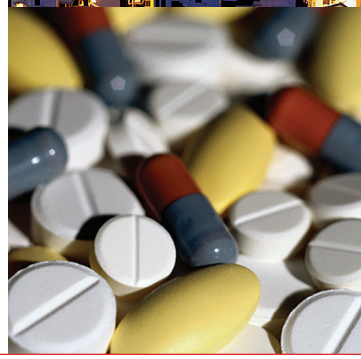

THE APPLICATION NOTEBOOK

Cover Photography: Getty Images

Comprehensive Analysis of C2–C8 PFAS Using a Novel LC Column

Restek Corporation

While not currently regulated, ultrashort-chain (C2–C3) per- and polyfluoroalkyl substances (PFAS) are of great interest. Current testing methodologies using reversed-phase liquid chromatography (LC) columns cannot be used because of a lack of retention, so either a separate method or a different column is required.

A unique, hybrid ion-exchange/HILIC column (Raptor Polar X) was used to develop a comprehensive LC–MS/MS method for the analysis of ultrashort-chain through long-chain, and alternative PFAS in water sources (tap, river, groundwater, and sewage effluent). The Raptor Polar X's multimode retention mechanisms allow for retention with a single isocratic run.

Experimental

Chromatographic conditions are reported in Figure 1.

To avoid introducing background contamination, polypropylene vials and caps were used during sample preparation.

Each water sample of 250 µL was mixed with 250 µL of methanol and 5 µL of internal standard solution (10 ng/mL of 13C2-PFHxA, 13C2-PFOA, 13C3-PFBS, 13C4-PFOS in methanol).

Calibration standards were prepared by using deionized water and fortified with 14 analytes (see Figure 1) at a range of 10–800 ng/L. The calibration standard solutions were diluted 1:1 as above.

A Restek tap water sample, along with three water samples (river, ground, and sewage effluent) supplied by the United States Environmental Protection Agency were fortified at 40 and 160 ppt. Blank and fortified water samples were diluted 1:1 in methanol as above for chromatographic analysis. For TFA measurement in groundwater, the sample was diluted fivefold with deionized water before fortification due to its high TFA concentration.

Results and Discussion

All analytes were eluted in 4 min with good peak shapes (Figure 1). The overall analytical cycle time was 8 min to ensure no matrix-related interferences.

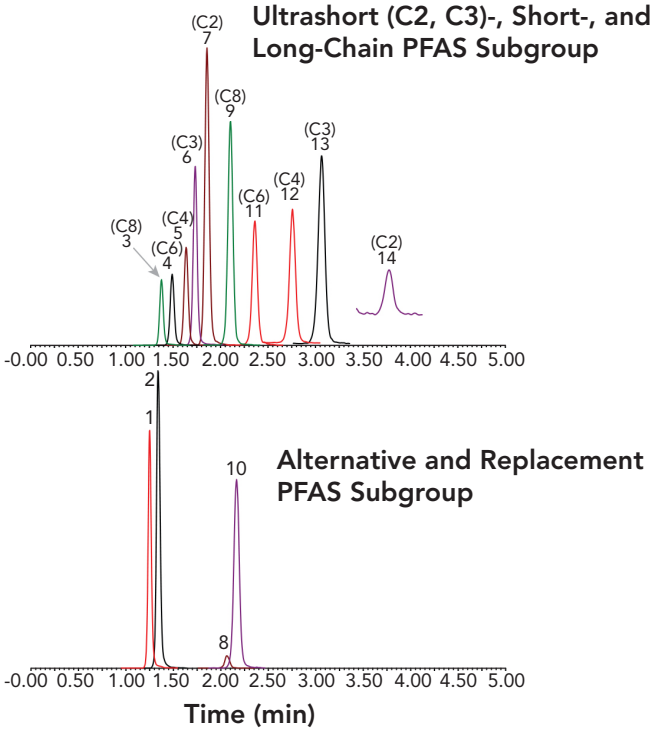

	Peaks	t_R (min)	Conc. (ng/L)	Precursor Ion	Product Ion
2	9-Chlorohexadecafluoro-3-oxanonane-1-sulfonate (9Cl-PF3ONS)	1.34	400	530.78	350.85
3	Perfluorooctanesulfonic acid (PFOS)	1.38	400	498.84	79.97
4	Perfluorohexanesulfonic acid (PFHxS)	1.49	400	398.9	79.97
5	Perfluorobutanesulfonic acid (PFBS)	1.64	400	298.97	79.97
6	Perfluoropropanesulfonic acid (PFPrS)	1.73	400	248.97	79.98
7	Perfluoroethanesulfonic acid (PFEtS)	1.86	400	198.98	79.92
8	Hexafluoropropylene oxide dimer acid (HFPO-DA)	2.06	400	284.97	168.92
9	Perfluorooctanoic acid (PFOA)	2.11	400	412.9	368.91
10	Ammonium 4,8-dioxa-3H-perfluorononanoate (ADONA)	2.15	400	376.9	250.93
11	Perfluorohexanoic acid (PFHxA)	2.36	400	312.97	268.9
12	Perfluorobutanoic acid (PFBA)	2.76	400	212.97	168.97
13	Perfluoropropionic acid (PFPrA)	3.06	400	163.03	119.01
14	Trifluoroacetic acid (TFA)	3.77	400	113.03	69.01

Column	Raptor Polar X (cat.# 9311A52)		**Detector**	MS/MS
Dimensions:	50 mm x 2.1 mm ID		Ion Mode:	ESI-
Particle Size:	2.7 µm		Mode:	MRM
Temp.:	40 °C			
			Instrument	UHPLC
Sample				
Diluent:	50:50 Water:methanol			
Conc.:	400 ng/L			
Inj. Vol.:	10 µL			
Mobile Phase				
A:	Water, 10 mM ammonium formate, 0.05% formic acid			
B:	60:40 Acetonitrile:methanol, 0.05% formic acid			
Time (min)	**Flow (mL/min)**	**% A**	**% B**	
0.00	0.5	15	85	
8.00	0.5	15	85	

Figure 1: Chromatogram of a 400 ng/L standard

Table I: Method accuracy and precision

	Average %Accuracy (%RSD)								
Matrices	**Tap Water**		**River Water**		**Groundwater****		**POTW Water**		**Deionized Watter**
Conc. (ng/L)	**40**	**160**	**40**	**160**	**40**	**160**	**40**	**160**	**10* (LLOQ)**
TFA	106 (16.9)	97.9 (7.10)	97.4 (10.8)	97.6 (6.12)	97.5 (14.5)	103 (8.87)	102 (17.1)	96.4 (7.33)	107 (3.55)
PFPrA	95.1 (4.08)	105 (3.48)	94.5 (6.85)	104 (2.36)	103 (9.37)	105 (8.34)	91.8 (4.90)	104 (7.09)	109 (1.61)
PFBA	106 (6.80)	117 (3.18)	105 (7.40)	114 (4.91)	111 (2.48)	120 (3.27)	106 (6.58)	114 (4.85)	104 (4.91)
PFHxA	93.3 (7.41)	111 (2.61)	91.8 (11.34)	103 (4.55)	102 (6.62)	109 (7.11)	103 (8.37)	108 (3.13)	115 (1.64)
PFOA	100 (4.24)	107 (3.14)	103 (6.71)	105 (2.64)	92.6 (3.85)	107 (3.09)	102 (4.57)	109 (3.64)	106 (3.28)
HFPO-DA	95.7 (11.9)	108 (9.05)	86.6 (8.97)	104 (5.45)	94.1 (18.6)	105 (9.35)	95.2 (8.49)	106 (9.23)	102 (16.8)
ADONA	106 (3.75)	116 (2.38)	100 (6.86)	110 (4.59)	104 (4.91)	113 (5.23)	111 (5.26)	115 (2.65)	105 (4.76)
PEEtS	94.8 (9.68)	110 (5.39)	89.4 (7.43)	102 (9.76)	96.5 (4.09)	108 (6.11)	104 (8.18)	109 (5.23)	99.8 (9.85)
PFPrS	104 (4.97)	115 (4.19)	95.0 (3.87)	107 (4.26)	106 (10.6)	114 (3.36)	111 (4.88)	114 (2.96)	108 (3.28)
PFBS	97.4 (10.1)	113 (3.97)	93.6 (5.24)	104 (4.19)	97.8 (4.47)	107 (4.23)	94.1 (10.7)	108 (4.48)	100 (11.0)
PFHxS	99.4 (15.7)	114 (3.56)	94.3 (9.79)	104 (5.28)	95.2 (5.63)	112 (3.20)	104 (8.19)	111 (4.07)	107 (11.7)
PFOS	104 (7.54)	107 (7.69)	103 (8.43)	105 (7.23)	97.3 (14.9)	110 (4.84)	109 (7.47)	108 (7.53)	102 (4.20)
9Cl-PF3ONS	98.7 (3.52)	105 (8.35)	91.8 (7.66)	103 (5.68)	94.7 (9.83)	105 (8.90)	105 (6.76)	107 (8.27)	107 (4.31)
11Cl-PF3OUdS	106 (10.1)	113 (3.54)	95.0 (3.52)	113 (8.15)	107 (6.61)	112 (4.54)	119 (4.25)	120 (9.10)	98.2 (11.3)

*20 ng/L LLOQ for TFA
**Groundwater was diluted fivefold for TFA only

Method linearity from 20–800 ppt for trifluoroacetic acid (TFA) and 10–800 ppt for all other analytes provided r^2 values >0.996 and deviations <20% using a 1/x weighted quadratic regression.

Samples were fortified at the low and high concentrations of their calibration ranges and run in duplicate for each analytical batch. A total of three batches were measured on different days. Concentrations of fortified samples were adjusted to account for any observed background contamination in sample blanks. Results are presented in Table I.

Conclusions

These results demonstrate that switching to a mixed-mode LC column provides the capability to analyze currently monitored and emerging PFAS contaminants in a single, short, isocratic run, preparing laboratories for the future of PFAS testing.

Restek Corporation
110 Benner Circle, Bellefonte, PA 16823
Tel. 1 (814) 353-1300
Website: www.restek.com

Extraction of Pesticides from Cannabis Flower and Edibles

Candice Cashman, Benedict Liu, and Alicia Stell, CEM Corporation

Cannabis and its products are on the road to being legalized throughout the United States. Because of the risk of pesticide exposure through inhaled and consumed cannabis products, the pesticides in the plant material and its products must be monitored. As matrices, cannabis and its related products have proven to be difficult to extract, and more traditional pesticide extraction methods, like QuEChERS, have been shown to perform poorly with these products. Thus, a better extraction method is needed. In this application note, in collaboration with SCIEX, the EDGE® was utilized to extract the Oregon pesticide list from cannabis flower and including edible cookies, chips, chocolate, hard candy, and granola bars. The average recoveries obtained were between 60% and 101%, and the average matrix effects were found to be between 70% and 130%. Thus, the EDGE is an excellent choice for laboratories extracting pesticides from cannabis and its products.

The use of cannabis and its products is growing more popular. With its continued legalization for recreational and medicinal use, it is subject to regulation, including monitoring its pesticide content. The presence of pesticides in cannabis is a concern because cannabis products are often inhaled or eaten, and with their consumption pesticides can bioaccumulate, causing potentially deleterious effects on human health. Because of these concerns, the list of pesticides monitored gets longer each year, and there is a need for good methods to extract and quantitate these compounds. Traditionally, the QuEChERS method has been used to extract pesticides from plants and food matrices, but cannabis and its products have shown time and again that cannabis is a difficult matrix to work with. Because of this, a simple, efficient method that produces high recoveries and repeatable results is still needed.

The EDGE is an extraction system that utilizes automation, heat, and solvent to extract samples quickly and effectively. It was used in a collaboration with SCIEX to extract pesticides from the Oregon list from cannabis edibles, including hard candy, chips, chocolate, cookies, and granola, and the cannabis flower. The average recoveries obtained for most pesticides in all the matrices were between 60% and 101%. The matrix effects were also assessed and found to be in the range of 70% to 130%. The EDGE offers cannabis laboratories an automated option for high recoveries with good matrix effects.

Materials and Methods

Extraction

Cannabis flower and cannabis cookies, chips, chocolate, hard candy, and granola bar were milled using a small coffee grinder. A portion of 300 mg of each matrix was weighed directly into a Q-Cup® containing a S1 Q-Disc® stack. The S1 Q-Disc stack is a sandwich of three filters including a glass-fiber filter surrounded by two cellulose filters. The samples were spiked with 150 ng of the Restek Oregon Pesticide Standards 1-6 (Catalogue numbers 32586, 32587, 32588, 32589, 32590, and 32591). A Q-Screen® was placed on top of each sample after spiking. The samples were loaded into an EDGE rack containing glass collection vials to collect the resulting extract. The samples were extracted using the indicated EDGE method. Five replicates of each sample type were extracted.

EDGE Method for Pesticides from Cannabis Flower and Edibles

Q-Disc: S1 Q-Disc stack (C9+G1+C9 sandwich)

Cycle 1

Extraction Solvent: Acetonitrile with 1.0% formic acid (v/v)

Top Add: 25 mL Bottom Add: 0 mL

Rinse: 5 mL Temperature: 40 °C

Hold Time: 02:00 (mm:ss)

Table I: Recoveries for each matrix

	Flower		Cookie		Chips		Chocolate		Hard Candy		Granola Bar	
Compound	Average	STDEV	Average	STDEV	Average	STDEV	Average	STDEV	Average	STDEV	Average	STDEV
Carbofuran	85.91	3.27	94.96	3.53	78.92	7.23	88.79	4.90	88.66	8.19	95.27	3.14
Cyantraniliprole	83.04	10.36	112.85	12.02	99.83	2.19	98.30	7.25	105.32	7.25	103.65	5.38
Cypermethrin	99.17	2.30	100.65	3.52	85.04	5.24	96.40	0.99	96.90	5.24	100.88	3.71
Fenproximate	107.80	2.60	91.93	3.13	75.40	8.68	82.81	3.29	86.90	6.43	89.83	6.06
Methiocarb	80.07	10.50	91.21	6.01	74.71	2.92	85.93	2.35	86.22	4.65	91.42	1.68
Permethrin trans	95.22	3.63	83.00	5.88	70.42	4.37	83.11	4.35	82.65	3.23	84.20	2.92
Piperonyl Butoxide	92.99	2.99	87.46	2.09	72.36	1.85	80.36	3.05	84.78	3.63	84.04	1.50
Prallethrin	74.13	3.07	113.83	8.00	73.16	5.70	79.79	8.38	86.38	4.66	82.38	4.42
Spirotetramat	84.46	6.98	92.92	6.79	82.29	5.47	91.55	3.80	90.31	9.75	92.30	3.66
Thiacloprid	83.92	6.06	93.29	3.67	79.20	3.44	87.78	6.41	91.28	3.25	90.92	4.89

Table II: Matrix effects for each matrix

	Flower		Cookie		Chips		Chocolate		Hard Candy		Granola Bar	
Compound	Average	STDEV	Average	STDEV	Average	STDEV	Average	STDEV	Average	STDEV	Average	STDEV
Carbofuran	90.58	5.36	89.32	7.20	100.89	6.84	98.02	6.59	94.61	6.59	87.52	10.30
Cyantraniliprole	95.37	14.80	98.47	20.84	96.83	14.91	94.18	14.82	101.66	13.80	99.17	18.02
Cypermethrin	87.80	15.82	100.03	3.56	100.22	6.58	99.14	16.24	93.85	3.44	91.84	11.26
Fenproximate	76.36	14.15	89.54	9.36	98.32	10.72	91.65	17.34	96.04	4.94	93.05	15.07
Methiocarb	83.80	9.04	92.51	9.94	92.54	3.28	95.97	10.33	90.90	5.91	89.86	10.60
Permethrin	106.56	18.41	102.58	8.25	95.66	4.08	97.58	18.02	96.16	3.71	91.17	11.10
Piperonyl Butoxide	88.86	6.91	102.17	4.76	100.36	5.26	101.12	7.28	101.16	2.23	97.37	13.02
Prallethrin	91.02	5.95	120.04	3.22	99.79	6.74	100.86	7.33	104.36	6.77	94.74	15.34
Spirotetramat	90.86	8.20	100.20	9.93	100.66	3.88	113.34	8.95	100.83	5.55	97.97	11.87
Thiacloprid	98.23	3.51	104.65	9.67	101.91	6.39	104.00	3.33	95.47	9.54	95.81	17.09

Wash 1
Wash Solvent: Acetonitrile with 1.0% Formic Acid (v/v)
Wash Volume: 15 mL
Temperature: 40 °C
Hold Time: 00:30 (mm:ss)
Wash 2
Wash Solvent: Acetonitrile with 1.0% Formic Acid (v/v)
Wash Volume: 15 mL
Temperature: - - - Hold Time: - -:- -

Post-Extraction

The extracts were placed in a -20 °C freezer for 2 h as part of the winterization process. The lipids present in the sample created a flocculant, and the remaining extract was poured into another vial for analysis.

Analysis

For recovery analysis, the extracts were directly injected. Electrospray ionization (ESI) was used for all analytes except for chlorfenapyr for which atmospheric pressure chemical ionization (ACPI) was used. Analytes were separated using a Phenomenex Luna Omega Polar C18 column (150 × 4.6 mm, 3 µm). The injection volume was 1 µL. For ESI the mobile phases were A: water with 5 mM ammonium formate and 0.1% formic acid and B: methanol with 5 mM ammonium formate and 0.1% formic acid. For ACPI the mobile phases were: A: water and B: acetonitrile. The samples were analyzed using previously determined MRM transitions for each pesticide on a SCIEX Triple Quad™ 7500 LC–MS/MS.

Results

The recoveries were determined using solvent-matched calibration curves. An abbreviated set of recoveries with their respective standard deviations can be found in Table I. The average recoveries for all matrices were mostly within the range 60% to 101%, which is generally the ideal range for recoveries. The standard deviations of the recoveries for almost all compounds were below 15%, which is also ideal.

The matrix effects were also assessed by comparing the extract of each blank matrix spiked with the pesticides at the initial spiking conditions to neat standard. The abbreviated set of matrix effects with their standard deviations are shown in Table II. The matrix effects were found to be in the range 70% to 130%. The flower matrix showed the most variability in its matrix effects, with signal enhancement and suppression extremes. Propiconazole, spiromesifen, and acequinocyl were found to be suppressed in the flower matrix. The cookie, chocolate, and chip matrices had the least amount of variability, with a tighter distribution overall.

To view the entire set of pesticides extracted from this study please download the full application note at https://cem.com/en/the-extraction-of-pesticides-from-cannabis-flower-and-edibles.

Conclusion

With the expanding cannabis industry within the United States, testing laboratories are monitoring cannabis and its products for pesticide content. Traditional pesticide extraction methods, like QuEChERS, have shown to work poorly with cannabis plant and cannabis edibles. Therefore, new and better extraction methods are needed. Within this work, in a partnership with SCIEX, the EDGE was used to extract pesticides from the Oregon List from cannabis flower and the edibles cookies, chips, chocolate, hard candy, and granola bar. The determined recoveries found for all pesticides, except spinosad, in all matrices were between 60% and 101%, which is well within the desired range, and all the recoveries, except for that of daminozide, methyl parathion, and imidacloprid, had standard deviations below 15%. The matrix effects for each matrix were found to be 70% to 130%. Thus, these data indicate that the EDGE is an excellent choice for the extraction of pesticides from cannabis material and edibles.

We would like to thank our collaborators at SCIEX for extracting these samples on the EDGE and analyzing the results.

CEM Corporation
P.O. Box 200, Matthews, NC 28106
tel. (704) 821-7015, (800) 726-3331, fax (704) 821-7894
Website: www.cem.com

The Chiral Separation of Remdesivir and Several of its Key Starting Materials

Weston J. Umstead, Chiral Technologies, Inc.

The start of 2020 saw the outbreak of the COVID-19 pandemic, and almost immediately, the search for a viable vaccine candidate, and effective treatments for those diagnosed with the virus, began. One of the compounds that emerged early on for the treatment of COVID-19 patients was remdesivir, an antiviral drug manufactured by Gilead Sciences. Studies conducted since its initial implementation have confirmed its effectiveness in shortening the recovery times of patients hospitalized, and in lowering the overall mortality rate from the disease.

The synthesis of remdesivir was well documented in the literature, however there are a few key chiral intermediates in the synthesis that were not previously well resolved under high-performance liquid chromatography (HPLC) conditions. The chiral separations of these compounds (shown in Figure 1 along with remdesivir itself) is shown on two Daicel immobilized chiral stationary phases (CHIRALPAK® IA-3 and CHIRALPAK IG-U), as well as on one of Daicel's achiral columns, DCpak® PTZ. The separation of remdesivir is also shown on CHIRALPAK IA-3 under normal-phase HPLC conditions.

Discussion

The two phosphoramidite starting materials contain two chiral centers, one on the phosphorus and the other on the carbon alpha to the phosphoramidite functional group. Therefore, the goal was to develop a separation, that could

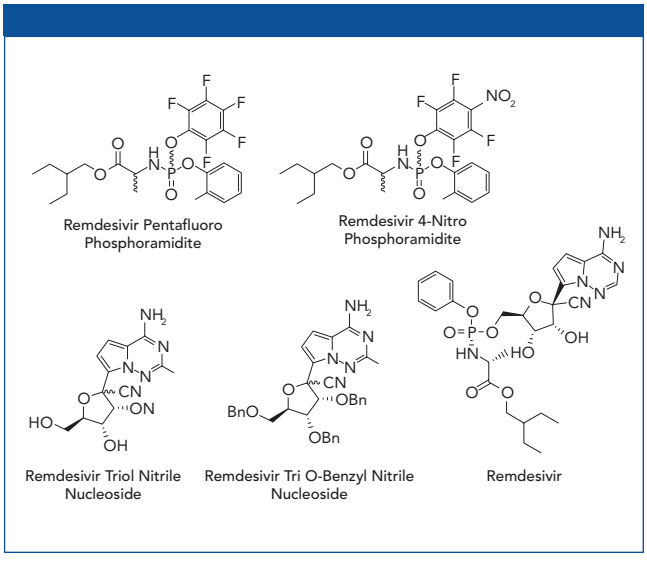

Figure 1: Remdesivir and its key starting materials

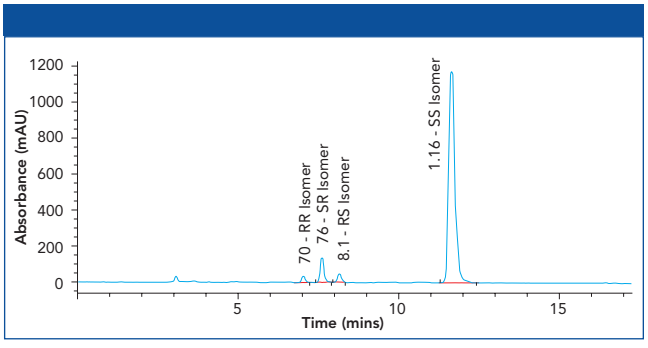

Figure 2: Separation of remdesivir pentafluoro phosphoramidite KSM

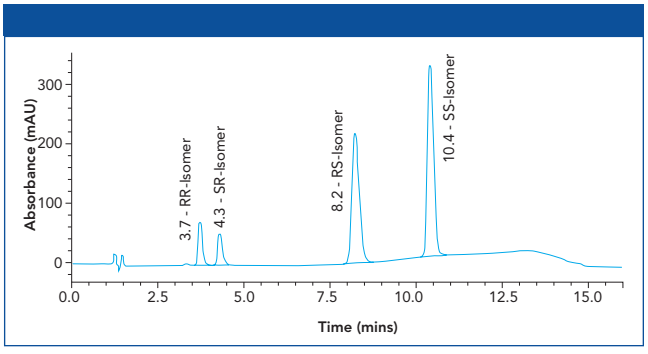

Figure 3: Separation of remdesivir 4-nitro phosphoramidite KSM

Table I: Chromatographic conditions for the separation of remdesivir pentafluoro phosphoramidite KSM

Column	CHIRALPAK® IA-3 (250 mm × 4.6 mm i.d.)
Mobile Phase	90-10 = n-Hex-IPA (v/v)
Flow Rate	1.0 mL/min
Detection	210 nm ref. 450 nm
Temperature	25 °C
Sample	1.0 mg/mL solution in mobile phase
Injection Volume	10 µL

quantify all four potential isomers. For the pentafluoro analog, a normal phase screening across Daicel's library of immobilized chiral stationary phases (CSPs) yielded a very nice resolution on CHIRALPAK IA-3 (Figure 2). No additional optimization from this initial screening was required.

The 4-nitro analog was a bit more challenging, as no viable separations on normal phase were initially found. However reversed-phase screening using a water/MeOH gradient

Table II: chromatographic conditions for the separation of remdesivir 4-nitro phosphoramidite KSM	
Column	CHIRALPAK® IG-U (100 mm × 3.0 mm i.d.)
Mobile Phase	Mobile phase A: water/methanol = 5/95 (v/v) Mobile phase B: acetonitrile Time (min)/%B: 0/0, 3/0, 10/35, 11/0, 16/0
Flow Rate	0.4 mL/min
Detection	270 nm ref. 450 nm
Temperature	40 °C
Sample	1.0 mg/mL solution in ACN/water = 30/70 (v/v)
Injection Volume	3 µL

Table III: chromatographic conditions for the separation of remdesivir triol nitrile and tri o-benzyl nitrile nucleoside KSM	
Column	DCpak® PTZ (150 mm × 4.6 mm i.d.)
Mobile Phase	Mobile phase A: 0.01% OPA in water Mobile phase B: methanol/acetonitrile = 10/90 (v/v) Time (min)/%B: 0/90, 15/50, 20/50, 20.1/90, 25/90
Flow Rate	1.0 mL/min
Detection	245 nm ref. 450 nm
Temperature	40 °C
Sample	0.5 mg/mL solution in methanol/water = 90/10 (v/v)
Injection Volume	10 µL

Table IV: chromatographic conditions for the separation of remdesivir	
Column	CHIRALPAK® IA-3 (250 mm × 4.6 mm i.d.)
Mobile Phase	n-hexane/ethanol/IPA/ethanolamine/formic acid = 80/5/15/0.05/0.1 (v/v/v/v/v)
Flow Rate	1.5 mL/min
Detection	245 nm ref. 450 nm
Temperature	40 °C
Sample	1.0 mg/mL solution in hexane/ethanol = 50/50 (v/v)
Injection Volume	10 µL

yielded a partial separation for two of the four expected peaks. The addition of acetonitrile as a mobile phase component resulted in better selectivity and thus a separation of the final two, earlier eluting isomers (Figure 3).

The separation of the triol and tri o-benzyl nitrile starting materials is a chiral/achiral separation, which can be accomplished on a Daicel polysaccharide CSP. However in this case, Daicel's HILIC DCpak PTZ column was used. The initial screening was performed without the addition of any additives, however the peak shape was less than desirable. The addition of 0.01% o-phosphoric acid to the mobile phase A component had a significant improvement to the peak shape, and optimization of the gradient led to a baseline resolution of all four isomers (Figure 4).

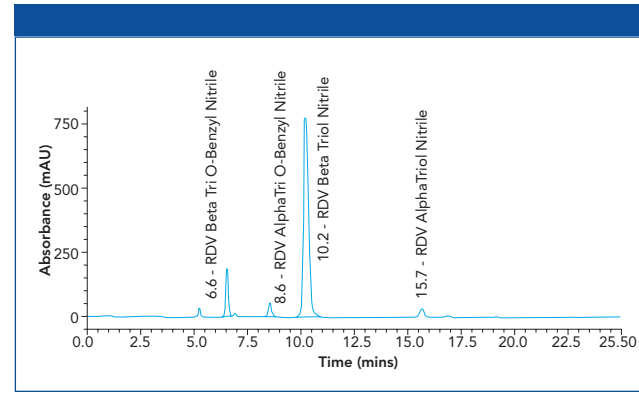

Figure 4: Separation of remdesivir triol nitrile and tri o-benzyl nitrile KSM

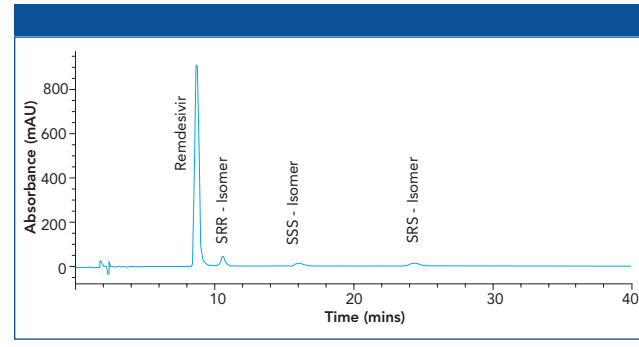

Figure 5: Separation of remdesivir

Lastly, remdesivir was screened, and a good separation under normal-phase conditions was observed, with slightly undesirable peak shape. Because the compound contains both basic and slightly acidic functional groups, the addition of both ethanolamine and formic acid was able to sharpen the peaks, and the combination of isopropanol and ethanol gave a nice compromise between selectivity and retention.

Chiral Technologies, Inc.
1475 Dunwoody Drive, Suite 310, West Chester, PA 19380
Tel. (610) 594–2100
Website: www.chiraltech.com

Analysis of Redox and Bioenergetics Metabolites with Polymeric iHILIC®-(P) Classic HILIC Column and Mass Spectrometry

Susan Kim*, Wen Jiang†, and Joshua D. Chandler*‡,
*Department of Pediatrics, Division of Pulmonology, Allergy & Immunology, Cystic Fibrosis and Sleep Medicine, Emory University, Atlanta, Georgia †Hilicon AB ‡Children's Healthcare of Atlanta, Atlanta, Georgia

Aerobic organisms use oxygen as the terminal electron acceptor in cellular respiration. Molecular oxygen is capable of accepting up to four electrons to become water through the reaction catalyzed by mitochondrial complex IV (1). However, intermediate reactive oxygen species (ROS) are formed by partial reduction of oxygen. Aerobes have evolved both physiological and biochemical strategies to mitigate molecular damage caused by ROS while maintaining oxygen availability for cellular respiration (2). Core metabolism and redox control depend on a number of metabolites, including nucleotides ($NADP^+$/NADPH and NAD^+/NADH) and redox-active amino acids and peptides (particularly glutathione, cysteine, and methionine). For example, reduced glutathione (GSH; γ-L-glutamyl-L-cysteinylglycine) is an important regulator of local hydrogen peroxide signalling by serving as a cofactor of glutathione peroxidases (3). In turn, oxidized glutathione (GSSG) is reduced back to GSH in an NADPH-dependent fashion by GSSG reductase (4). Both cysteine and methionine in proteins may act as redox switches linked to NADPH-dependent repair mechanisms (5,6). NADPH is generated by the pentose phosphate pathway that links to glycolysis, which generates ATP and relies on NAD^+ as a cofactor. Multiple steps of the citric acid cycle generate NADH that supports chemiosmotic ATP synthesis.

Liquid chromatography–mass spectrometry (LC–MS)-based metabolomics present an opportunity to monitor many molecules simultaneously, relying on a combination of chromatographic and mass-based resolution to quantify hundreds to thousands of molecules in a typical experiment (7). However, many of the metabolites noted above could be challenging to profile simultaneously because of poor chromatographic separation or peak shape (8). We sought to develop a simple method using hydrophilic interaction liquid chromatography (HILIC) that could simultaneously profile the metabolites that are important in redox regulation and bioenergetics. By incorporating these metabolites into a nontargeted-compatible and derivatization-free approach, information about redox and bioenergetics can be gained as part of routine profiling.

Experimental

LC–MS System: A Vanquish Horizon binary pump was hyphenated to a Q Exactive HF (Thermo Fisher Scientific), set at 120,000 FWHM, 1e6 AGC target, and 200 ms max IT. Connecting tubings between the column, autosampler, and MS system were 100 µm i.d. PEEK-lined stainless steel MarvelXACT tubing (IDEX Health & Science) instead of original Viper MP35N. The HESI-II probe was held at 320 °C and +3.5 kV with 40 sheath gas, eight auxiliary gas, and one sweep gas flow (arbitrary units).

Column: 150 × 2.1 mm, 5-µm, 200 Å, iHILIC®-(P) Classic (P/N 160.152.0520, Hilicon AB), coupled to a 20 mm guard column via a PEEK coupler.

Eluent: A) 15 mM ammonium acetate pH 9.4, B) acetonitrile.

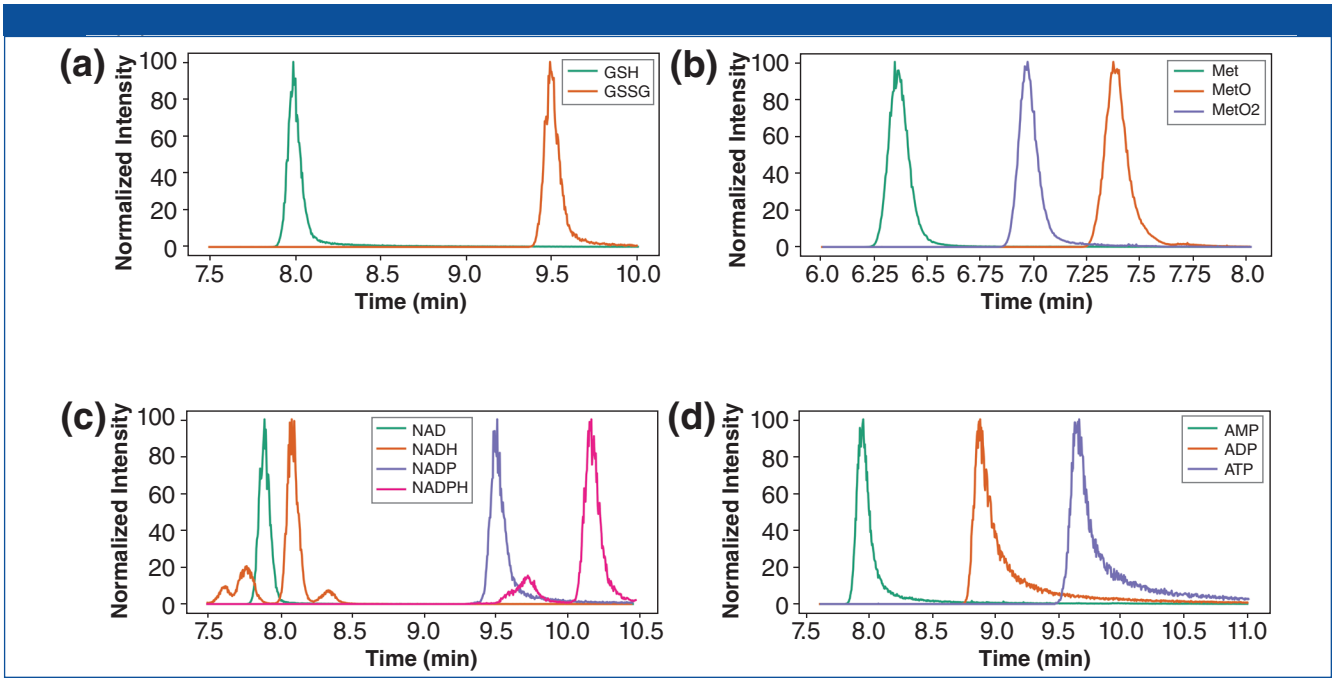

Figure 1: Base intensity-normalized chromatograms of (a) GSH/GSSG; (b) Met/MetO/$MetO_2$; (c) NAD^+/NADH/$NADP^+$/NADPH; (d) AMP/ADP/ATP.

Table I: Peak areas of reduced and oxidized compounds from reduced standards

	REDUCED	OXIDIZED	OXIDIZED %
GSH	6.82×10^{7}	2.16×10^{4}	0.03
METHIONINE	2.87×10^{8}	5.89×10^{5}	0.21
NADH	2.76×10^{7}	ND	NA
NADPH	8.32×10^{6}	ND	NA

*Metabolites were quantified in positive mode as their $[M+H]^+$ ions with 5 ppm mass accuracy. The result is based on a semi-quantitative comparison of peak areas.

Gradient Elution: 0–15 min, gradient from 10–90% A; 15–17 min, 90% A; 17–25 min, 10% A (column re-equilibration)
Flow Rate: 200 µL/min
Column Temperature: 40 °C
Injection Volume: 2.5 µL

Metabolite Samples: Individual metabolites were prepared fresh from reference standards in water (50 µmol/L). We focused on the following 14 metabolites: oxidized/reduced nicotinamide adenine dinucleotide (NAD^+/NADH), oxidized/reduced nicotinamide adenine dinucleotide phosphate ($NADP^+$/NADPH), adenosine mono-/di-/triphosphate (AMP/ADP/ATP), glutathione/glutathione disulfide (GSH/GSSG), methionine/methionine sulfoxide/methionine sulfone (Met/MetO/$MetO_2$), and cysteine/cystine (Cys/CySS). We also analyzed human plasma Standard Reference Material 1950 (MilliporeSigma) and metabolite extract of *E. coli* (Cambridge Isotope Labs), which were either reconstituted with a solution of 1:1:1 acetonitrile–methanol–water + 8.33 µM D5-hippuric acid or extracted with addition of 2 vol 1:1 acetonitrile–methanol + 12.5 µM D5-hippuric acid followed by vortexing and incubation on ice for 30 min. Samples were then centrifuged at 20,000 *g* and 4 °C for 10 min. The supernatant was then applied for HILIC–MS analysis.

Results and Conclusion

The newly developed method provides excellent peak separation and overall good peak quality for all of the metabolites, as shown in Figure 1.

We analyzed all of the reduced metabolite standards to determine if autoxidation was rapidly occurring (Table I). Peak areas of most oxidized species from injections of reduced standards were <1% that of the reduced species at pH 9.4. However, in the case of the Cys standard, only oxidized CySS was detectible. When using neutral pH instead of 9.4, Cys was preserved and detected (though considerable autoxidation was still noted). Cys may be unstable at alkaline pH as a result of enhanced deprotonation to the nucleophilic thiolate form ($pKa = 8.3$) (3).

We then determined whether the 12 metabolites shown in Figure 1 were well represented in standard reference materials for untargeted metabolomics experiments. Human plasma SRM 1950 and the unlabelled *E. coli (Escherichia coli)* metabolite extracts were used as probes. Across the two matrices, signals for all metabolites except $NADP^+$ were observed (Table II).

This work demonstrates the feasibility of profiling core metabolites related to redox metabolism and bioenergetics, which might be incorporated into a nontargeted workflow for more extensive profiling.

Table II: Peak areas of metabolites in reference samples

	SRM 1950	*E. COLI*
GSH	1.06×10^{5}	9.89×10^{8}
GSSG	ND	8.92×10^{7}
METHIONINE	7.22×10^{7}	6.75×10^{7}
METO	5.75×10^{6}	1.48×10^{7}
$METO_2$	5.42×10^{5}	ND
NADH	ND	8.29×10^{4}
NAD^+	ND	1.42×10^{8}
NADPH	ND	2.01×10^{5}
$NADP^+$	ND	ND
ATP	ND	5.44×10^{6}
ADP	ND	1.46×10^{7}
AMP	ND	5.11×10^{7}

*Metabolites were quantified in positive mode as their $[M+H]^+$ ions with 5 ppm mass accuracy.

We note that thiol metabolites are labile and nontargeted profiling of these should be experimentally validated with derivatization-based methods (9). A HILIC method with an acidic mobile phase may offer better stability for thiol compounds as well.

Acknowledgements

JDC gratefully acknowledges grants from the National Institutes of Health (HL150658 and NR018666) and Cystic Fibrosis Foundation (TIROUV19A0) and startup funds from the Pediatric Center of Georgia.

References

(1) P.M. Wood, *Biochem. J.* **253**(1), 287–289 (1988).
(2) H. Sies *et al.*, *Annu. Rev. Biochem.* **86**, 715–748 (2017).
(3) C.C. Winterbourn and M.B. Hampton, *Free Radic. Biol. Med.* **45**(5), 549–561 (2008).
(4) A. Meister and M.E. Anderson, *Annu. Rev. Biochem.* **52**, 711–760 (1983).
(5) Y.M. Go et al., *Free Radic. Biol. Med.* **84**, 227–245 (2015).
(6) S. Boschi-Muller and G. Branlant, *Bioorg. Chem.* **57**, 222–230 (2014).
(7) S.P. Putri and E. Fukusaki, *Mass Spectrometry-Based Metabolomics* (CRC Press, 2016).
(8) J.L. Spalding et al., *J. Proteome Res.* **17**(10), 3537–3546 (2018).
(9) J.M. Johnson et al., *Clin. Chim. Acta* **396**(1–2), 43–48 (2008).

Hilicon AB
Tvistevägen 48 A, SE-90736 Umeå, Sweden
Tel.: +46 (90) 193469
E-mail: info@hilicon.com
Website: www.hilicon.com

Molecular Weight Determination of VLPs Using the LenS3 Multi-Angle Light Scattering Detector

Tosoh Bioscience LLC

Viruses and virus-like particles (VLPs) are multimeric protein structures that mimic native viruses but are non-infectious. VLPs are subjects of interest, as their potential continues to grow as candidates in new vaccines and gene therapy products. For example, commercially available VLP-based vaccines are available for hepatitis B and human papillomavirus. Robust analytical techniques are needed to not only ensure quality of final products but provide data for informed decision-making during the development process.

Size-exclusion chromatography (SEC) is an analytical technique that provides results on the size and purity of macromolecules. When coupled with multi-angle light scattering (MALS), it offers both molecular weight (MW) and radius of gyration (R_g or size). Importantly, AU_{280} detection is only concentration dependent, whereas MALS corresponds to both concentration and molecular weight. Thus, the large molecular weight characteristic of VLPs inherently provides MALS with a strong scattered-light response and enables VLP detection even in a dilute solution that is well below the AU_{280} detection limit.

The primary challenge in the analysis of very large macromolecules by SEC is the selection of the appropriate analytical column. Here we explore the TSKgel® PWXL series of SEC columns, which includes a wide range of different pore sizes on a polymethacrylate stationary phase, for their utility in the analysis of large macromolecules such as VLPs. The protein calibration curves (Figure 1) show the separation range of TSKgel PWXL columns. The majority of VLPs have a molecular weight of >1 megadaltons (MDa), which make the TSKgel G5000PWXL (100 nm pore size), TSKgel G6000PWXL (>100 nm pore size) and TSKgel GMPWXL (mixed bed) ideal columns of choice for analysis of VLPs.

Materials and Methods

Columns:	TSKgel GMPWXL, 13 µm, 7.8 mm ID × 30 cm TSKgel G5000PWXL, 10 µm, 7.8 mm ID × 30 cm
Instrument:	Thermo Scientific UltiMate® 3000
Mobile phase:	0.145 mol/L NaCl, 0.01 mol/L HEPES, 0.05% sodium azide, pH 7.4 (refractive index, 1.333)
Flow rate:	0.3 mL/min or as indicated
UV:	UltiMate 3000 multiple wavelength detector
RI:	Shodex RI-504 semi-micro RI detector
MALS:	LenS3 MALS detector
Sample:	Parvovirus VLP (MVM-MVP) (Cygnus Technologies), stock 1×10^{12} particles/mL (10–15 µL injection), (dn/dc = 0.19, dA/dc = N/A)
MALS calibrant:	BSA, 5 mg/mL (dn/dc = 0.185, dA/dc 0.66)

In this application, parvovirus VLP was separately analyzed on both a TSKgel GMPWXL and TSKgel G5000PWXL SEC column coupled with the LenS3 MALS detector. Either RI or UV can function as the concentration detector. RI was used with the right angle light scattering signal (RALS) to measure MW. Extreme low angle (LALS), right angle, and extreme high angle (HALS) signals were used to plot angular dissymmetry and to determine R_g. The MALS detector was calibrated with BSA prior to sample analysis and all data were processed and analyzed using SECview® software.

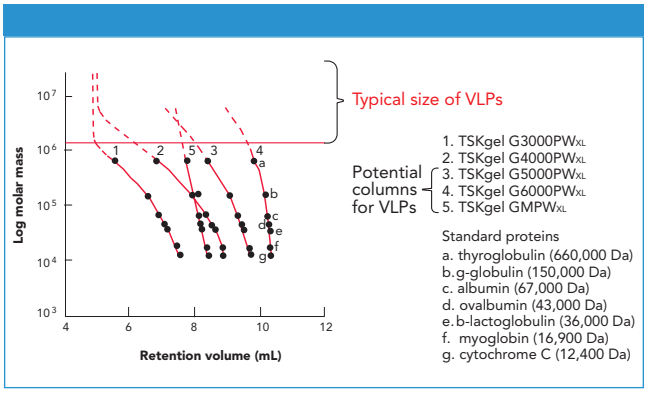

Figure 1: Protein calibration curves on TSKgel PWXL columns

Analysis of parvovirus VLP by SEC-MALS using the TSKgel GMPWXL column revealed a MW of ~4 MDa and R_g of 12.8 nm (Figure 2). These results closely align with reported values for this VLP (Biotech. Prog. 34, 1213–1220, 2018).

As seen in Figure 3, parvovirus VLP was diluted up to 64-fold and injected at 10 µL onto a TSKgel G5000PWXL column. Approximately 3×10^{10} particles per mL can still be detected using the RALS signal from the LenS3 MALS detector, which allows for analysis of materials with low concentration or when working with limited sample.

Conclusion

Mass spectrometry is the most common method previously used for VLP size determination, but this technique is costly and impractical for frequent analysis. Inclusion of SEC–MALS as an analytical technique to determine the MW and R_g is a preferred alternative, and allows for both routine analysis and process monitoring. The wide range in pore sizes and separation ranges of TSKgel PWXL SEC columns overcome challenges in analytical SEC where separations of large macromolecules require a larger pore-sized stationary phase. When these SEC columns are then combined with the greatly enhanced sensitivity of Tosoh Bioscience's LenS3 MALS detector, fast and easy analysis of MW and R_g with an improved level of detection (LOD) is provided.

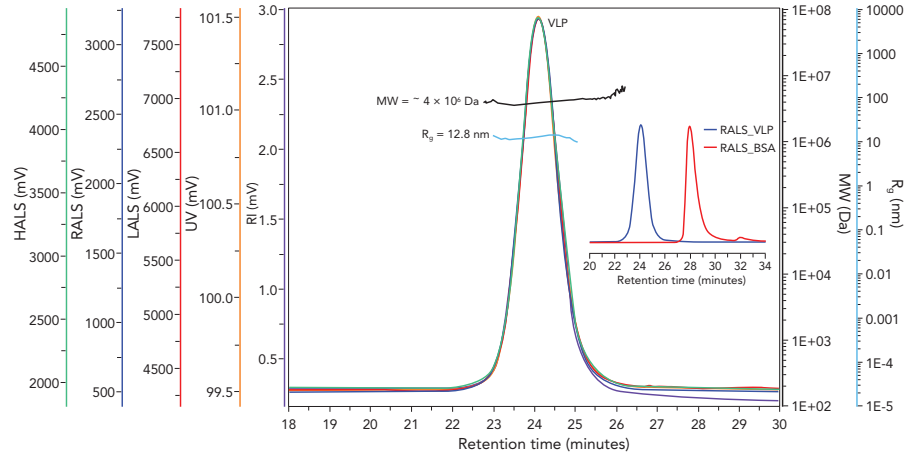

Figure 2: Analysis of parvovirus VLP and BSA on TSKgel GMPWXL mixed bed pore size SEC column

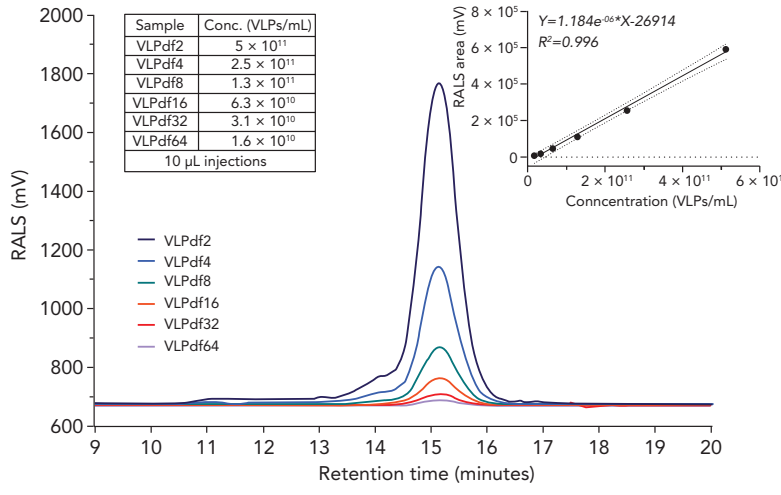

Figure 3: Limit of detection by RALS using TSKgel G5000PWXL at 0.5 mL/min

TOSOH BIOSCIENCE

Tosoh Bioscience LLC
3604 Horizon Drive, Suite 100, King of Prussia, PA 19406
Tel. (484) 805-1219, fax (484) 805-1277
Website: www.tosohbioscience.com

Polyurethane—Absolute Molar Mass by SEC–MALS

Wyatt Technology

Polyurethanes are typically analyzed by gel-permeation chromatography (GPC) or size-exclusion chromatography (SEC) using polymer standards and extensive column calibration. Besides being tedious, column calibration means that the resulting answers will be relative and not absolute, relying on the assumption that the reference standards have the same conformation, density and column interactions as the analyte of interest.

A far more effective means of characterizing polyurethanes involves adding multi-angle light scattering (MALS) to SEC, creating a SEC–MALS system that eliminates the need for column calibration and reference standards (1). SEC-MALS analyses derive from first principles; they are absolute and do not depend on such assumptions.

Materials and Methods

A polyurethane sample was dissolved in DMF with 0.01 M LiBr. The specific refractive index increment, dn/dc, was measured off-line by injecting aliquots at a series of carefully prepared concentrations into an Optilab differential refractometer (Wyatt Technology). The Optilab uses a light source at the same wavelength as the DAWN multi-angle light scattering detector (Wyatt Technology), for the measured dn/dc value to provide maximal accuracy in concentration and MALS analyses.

An aliquot was then injected onto the SEC column at a flow rate of 0.485 mL/min. The eluting fractions were characterized by the DAWN and Optilab to determine the molar mass of each one-second slice.

Results and Discussion

The following results—courtesy of Kolon Corp., Korea—display the absolute molar mass at each slice in the light scattering chromatogram (Figure 1) and the conversion to a differential distribution (Figure 2). The logarithmic relationship displayed between molar mass and elution volume provides clear indication that the separation is ideal that and no unexpected column interactions occur.

The results are further analyzed to produce the absolute weight-average molar mass M_w, other molecular weight moments of the peak, and the polydispersity M_w/M_n. These are shown in Table I, as are the uncertainties of each of the calculated quantities.

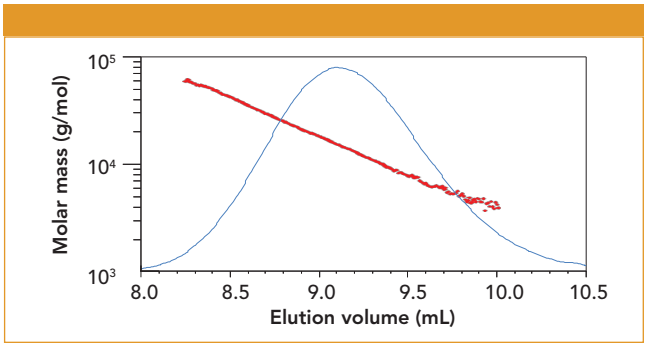

Figure 1: A plot of the molecular weight vs. volume for the polyurethane sample overlaid upon the trace from the 90° light-scattering detector.

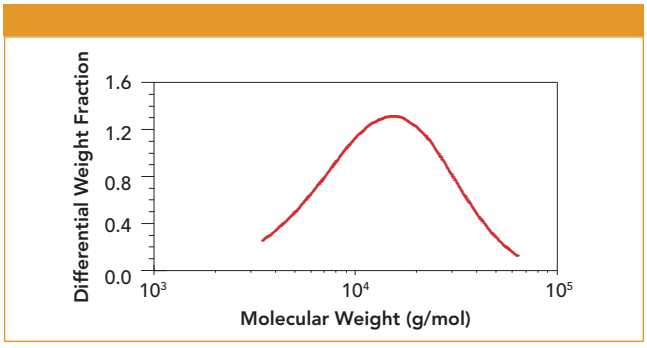

Figure 2: The differential molecular weight distribution of this polyurethane ranges from about 4 kDa to more than 60 kDa.

Table I: Molar mass and polydispersity results from SEC-MALS

Property	Value
Peak range	8.25 - 10.00 mL
Injected mass	2.058×10^{-4} g
Mn - number-average MW	$(1.36\pm0.03) \times 10^4$ g
Mw – weight-average MW	$(2.02\pm0.02) \times 10^4$ g
Mz – z-average MW	$(2.87\pm0.05) \times 10^4$ g
Polydispersity Mw/Mn	1.49±0.04

Conclusions

Although standard GPC is considered to be the primary technique for determination of molar mass distributions, only SEC–MALS provides unbiased and absolute molar mass measurements. Simply adding a MALS instrument to an existing GPC system reveals new horizons in absolute polymer characterization.

Reference

(1) P.J. Wyatt,. *Anal. Chim. Acta*, **272,** (1993).

Wyatt Technology Corporation
6330 Hollister Avenue
Santa Barbara, CA 93117-3115
Website: www.wyatt.com

FUNDAMENTALS

Controlling Retention Time Drift in Industrial Chromatography

Brian Rohrback

For argument's sake, I will forward two 80:20 observations that apply to chromatography:

- 80% of published applications are for research and development (R&D) studies, and 20% are for routine applications
- 80% of all chromatographs sold are for routine work, and 20% go to the R&D labs.

While not surprising, it means that chromatographers, often ignore issues that are critical in routine, industrial settings that should see more of our light. So, think about it: Most chromatographs are tasked on day one with a specific analysis and, 20 years later, their final analysis will be the same as the first.

Deploying a chromatograph in a quality control (QC) or process setting is critical to many complex streams in that it provides detailed information on the composition of a huge array of mixtures and provides the means of integrating compositional control strategies in the plant. Day-to-day and instrument-to-instrument variability will frustrate data analysis. Computer-enabled technology can be applied to mitigate the impact of aging instruments and instrument differences, leading to a more robust, lower-maintenance world for industrial chromatographs. The key issue is to control retention time drift.

Because peak retention on the column has some variability, this shifting increases the likelihood of misidentifying a peak and, ultimately, risks misreporting a component's concentration. Chromatographic retention time drift from run-to-run is always present, but usually is not a significant source of variability. Over time, however, any retention drift amplifies the risk of an error in peak identification, which can lead, in turn, to mistakes in peak tables or in evaluating the overall distribution. Software control of retention time drift is a generic solution to this problem and addressing retention time variation simplifies ownership of a chromatograph by making the data consistent from one month to the next, even one instrument to the next.

In 1965, Kováts described how you can use peaks that are easily identified as markers to calculate relative retention times of neighboring peaks (1). In the late 1990s, groups worked to address the problem of retention time variability by borrowing a multivariate technology that had been applied to voice recognition; one example is correlation optimized warping (COW) described by Nielsen (2). Software, both commercial and freeware, has been available for these approaches since the early 2000s. My team has employed both techniques, separately and in combination, for two decades or so, and has used alignment technology to manage a variety of routine and complex applications, including clinical analysis for the Centers for Disease Control (CDC), systems for economic fraud investigations for the U.S. Food and Drug Administration (FDA), and process hydrocarbon evaluations in refineries and chemical plants.

The traditional way of handling this situation is to rerun the standard and accept new time positions for the peaks. This approach gives a very short-term context and, by forcing frequent recalibrations, lowers the number of samples that can be processed. Hands-on recalibration makes the system more unreliable online, where it is harder to attend to these changes. We often relegate this type of analysis to a supervised laboratory rather than placing it in a less-supervised position near the sampling point, where the feedback would be timely.

But what if we could rely on retention times not changing? This is an example of where chemometric alignment technology should be used. For software alignment to work, one chromatogram must be previously chosen to be the alignment standard; the algorithm then adjusts the peak positions in all the other traces to match that standard as closely as possible. COW-based alignment does not require the alignment standard to be run close to the analysis date, nor does it even need to be run on the same chromatograph. In practice, alignment keeps the peaks in place for a significantly longer time and reduces the work necessary to keep the system calibrated.

The idea that a small amount of software can be added to a chromatographic data system and have that addition open a true plug-and-play capability for the instrument and application is very powerful. Ostensibly, a company could keep a cold spare chromatograph in inventory. When a process or laboratory unit goes down for any reason, the storage unit would be placed online and have its data be completely comparable to all previous runs on its very first injection, possibly without ever performing a traditional calibration. Alignment can also apply this procedure to the historical chromatographic data assembly, resulting in a consistent database ready to be mined.

This conclusion also holds for situations where the column and the method conditions are similar. But if this is the case, the ability to perform more complex chromatographic evaluations in a fully automated manner is achieved.

References

(1) E. Kováts, *Adv. Chromatogr.* **1,** 229–247 (1965).

(2) N-P. V. Nielsen, J.M. Carstensen, and J. Smedsgaard, *J. Chromatogr. A* **805,** 17–35 (1998).

Brian Rohrback is the President and CEO of Infometrix, in Bothell, Washington. This article is a collaboration between *LCGC* and the American Chemical Society Analytical Division Subdivision on Chromatography and Separations Chemistry.

BALTIMORE, MD

SEPTEMBER 13-15

BALTIMORE CONVENTION CENTER

THE WORLD'S LARGEST CANNABIS SCIENCE EVENT!

CANNABIS SCIENCE CONFERENCE

ANALYTICAL, MEDICAL, CULTIVATION & HEMP TRACKS

Come grow with us!

- ENHANCED SAFETY MEASURES
- SOCIAL DISTANCING ENFORCED
- HAND SANITIZING STATIONS
- CANNA BOOT CAMP
- PANEL DISCUSSIONS
- POSTERS & ORALS

and much more!

The CSC Events team hopes that you are healthy and safe and we are excited to get our community back together in 2021. Now more than ever advancing science and medicine and sharing our research is needed and we look forward to seeing you again soon!

"Cannabis Science Conference has proven to be among the most influential educational events in the movement. They assemble the brightest researchers in the world to teach patients & medical professionals sitting side-by-side, learning together. Cannabis Science Conference is helping to galvanize rigorous scientific data supporting cannabis as a medicine."

- Sue Sisley, MD

! Sponsorship and exhibition opportunities are available.
Please contact Andrea at Andrea@CannabisScienceConference.com for more info.

CannabisScienceConference.com

@CannabisScienceConference

@CannabisScienceConference

Raffinose Family of Oligosaccharides Separated on a Hamilton HC-75

Legumes, Blessing and Curse?

The Raffinose Family of Oligosaccharides (RFO) are low molecular weight non-reducing sugars. The sugars are connected through α-1, 6-galactosyl extensions of sucrose starting with Raffinose, Stachyose, and Verbascose. These highly water soluble sugars are universally distributed throughout the plant kingdom in roots, seeds, stems, tubers, and some leaves. RFOs are most commonly found in dehydrated legumes, like lentils, soybeans, and chickpeas, and are thought to exist mainly to protect the seed from degradation while awaiting optimal germination conditions. RFO consumption is not generally considered nutritional due to the indigestibility of α-galactosidic linkages by monogastric animals which include humans. When large amounts of under hydrated legumes are consumed by monogastric animals, multiple breakdown pathways are initiated. The gut breaks the molecules down into gases, primarily hydrogen, carbon dioxide, small amounts of methane, and short chain fatty acids.[1] The large production of gastric gasses leads to an increase in osmotic pressure in the gut and promotes diarrhea, cramps, bloating, and overall discomfort.

As such, RFO's have generally been considered to have low nutritional value. However, studies have shown that if consumed in small quantities, < 3 g/day, positive effects occur.[2] Of these, lowered blood pressure, an increase in the production of butyrate and propionate from the gut which promote healthy brain activity, and has been shown to reduce the instance of colorectal cancer.[3]

Bifidobacterium and lactobacilli concentration are shown to increase (indicated as beneficial microbiota produced from consumption of RFO's) and aid the production of short chain fatty acids, reduce gut pH, and increase the production of acetic and lactic acid which reduces pathogenic bacteria in the gut. Interestingly, various food manufacturers are now taking advantage of the beneficial aspects of bifidobacteria due to its role in colonic health.[4]

Analysis of these compounds are not easily accomplished using the more chromatographically prevalent methods (reversed-phase or ion exchange). Owing to the polar nature of this family of oligosaccharides, the Hamilton HC-75 (Ca^{2+}) gel matrix column was chosen. The HC-75 series uses a ligand exchange mechanism in order to interact more or less strongly with the analytes of interest. As the oligosaccharide structure increases, less optimal interaction with the exchange metal occurs resulting in a retention decrease, ending with semi overlapping peaks corresponding to the longer oligosaccharides of n = 4 and 5. In this series of saccharides, the calcium form provided the best separation. Better resolution was achieved with lower flow rates but at the cost of peak shape and time. An added advantage of the HC-75 matrix is that the mobile phase consists only of water. In this application we utilized refractive index as the detector, but conductivity or electrochemical detection can be used with good results.

Column Information

Packing Material	HC-75 (Ca^{2+}), 9 µm
P/N	79436

Chromatographic Conditions

Gradient	Isocratic
Temperature	80 °C
Injection Volume	10 µL
Detection	Refractive Index
Dimensions	305 x 7.8 mm
Eluent A	DI Water
Flow Rate	0.6 mL/min

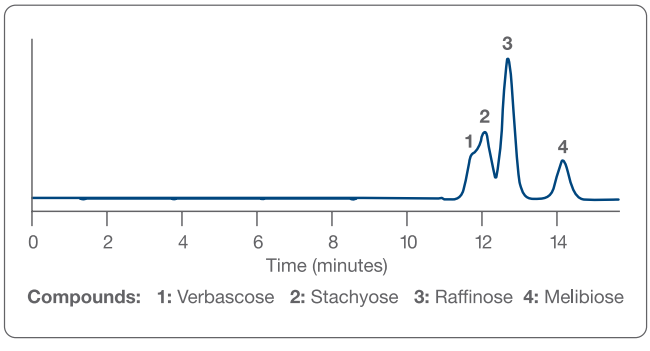

Compounds: **1:** Verbascose **2:** Stachyose **3:** Raffinose **4:** Melibiose

1) *Cristofaro E., Mottu F., Wuhrmann J.J., Nestle Res. News, 1973, 102–104.*

2) *Martínez-Villaluenga C., Frias J., Vidal-Valverde C., Crit. Rev. in Food Sci. and Nut., 2008, 48:301–316.*

3) *Bruno-Barcena J.M., Azcarate-Peril M.A. J Funct Foods, 2015, 12:92–108. Martínez-Villaluenga C., Gómez R., Frias J., Vidal-Valverde C., J. Food Prot., 2005, 68:1246–1252.*

Author: *Adam L. Moore, PhD, Hamilton Company*

For more information on Hamilton HPLC columns and accessories or to order a product, please visit **www.hamiltoncompany.com** or call **(800) 648-5950** in the US or **+40-356-635-055** in Europe.

Lit. No. L80108 — 06/2020